Local Variational Quantum Compilation of Large-Scale Hamiltonian Dynamics

Kaoru Mizuta,[1,2,3,*] Yuya O. Nakagawa,[1] Kosuke Mitarai,[4,5,6] and Keisuke Fujii[3,4,5,7]

[1] *QunaSys Inc., Aqua Hakusan Building 9F, 1-13-7 Hakusan, Bunkyo, Tokyo 113-0001, Japan*

[2] *Department of Physics, Kyoto University, Kyoto 606-8502, Japan*

[3] *RIKEN Center for Quantum Computing (RQC), Hirosawa 2-1, Wako, Saitama 351-0198, Japan*

[4] *Graduate School of Engineering Science, Osaka University, 1-3 Machikaneyama, Toyonaka, Osaka 560-8531, Japan*

[5] *Center for Quantum Information and Quantum Biology, Osaka University, 1-2 Machikaneyama, Toyonaka, Osaka 560-0043, Japan*

[6] *Japan Science and Technology Agency (JST), Precursory Research for Embryonic Science and Technology (PRESTO), 4-1-8 Honcho, Kawaguchi, Saitama 332-0012, Japan*

[7] *Fujitsu Quantum Computing Joint Research Division at QIQB, Osaka University, 1-2 Machikaneyama, Toyonaka 560-0043, Japan*

(Received 12 April 2022; revised 5 July 2022; accepted 22 August 2022; published 5 October 2022)

The implementation of time-evolution operators on quantum circuits is important for quantum simulation. However, the standard method, Trotterization, requires a huge number of gates to achieve desirable accuracy. Here, we propose a local variational quantum compilation (LVQC) algorithm, which allows us to accurately and efficiently compile time-evolution operators on a large-scale quantum system by optimization with smaller-size quantum systems. LVQC utilizes a subsystem cost function, which approximates the fidelity of the whole circuit, defined for each subsystem that is as large as the approximate causal cones generated by the Lieb-Robinson (LR) bound. We rigorously derive its scaling property with respect to the subsystem size and show that the optimization conducted on the subsystem size leads to the compilation of whole-system time-evolution operators. As a result, LVQC runs with limited-size quantum computers or classical simulators that can handle such smaller quantum systems. For instance, finite-ranged and short-ranged interacting L-size systems can be compiled with $O(L^0)$- or $O(\log L)$-size quantum systems depending on the observables of interest. Furthermore, since this formalism relies only on the LR bound, it can efficiently construct time-evolution operators of various systems in generic dimensions involving finite-, short-, and long-ranged interactions. We also numerically demonstrate the LVQC algorithm for one-dimensional systems. Through the employment of classical simulation by time-evolving block decimation, we succeed in compressing the depth of the time-evolution operators up to 40 qubits by the compilation for 20 qubits. LVQC not only provides classical protocols for designing large-scale quantum circuits but also sheds light on applications of intermediate-scale quantum devices in implementing algorithms in larger-scale quantum devices.

DOI: 10.1103/PRXQuantum.3.040302

I. INTRODUCTION

The implementation of time-evolution operators under a large-scale Hamiltonian is one of the most important tasks in noisy intermediate-scale quantum (NISQ) devices [1] and larger fault-tolerant quantum computers to exploit their computational power. The task is computationally hard for classical computers; despite the enormous effort made toward its efficient computation, it generally takes resources that are exponential in their system size. On the other hand, quantum computers are capable of executing it in polynomial time [2]. It is also important for computing eigenvalues and eigenstates of a system on a quantum computer; the quantum phase-estimation algorithm [3–5] uses controlled time-evolution operators to generate them. Recent hardware with tens of qubits has realized its proof-of-principle demonstrations for systems such as Fermi-Hubbard models [6], discrete time crystals [7,8], and various equilibrium and nonequilibrium phenomena [9–11].

*kaoru.mizuta@riken.jp

Published by the American Physical Society under the terms of the Creative Commons Attribution 4.0 International license. Further distribution of this work must maintain attribution to the author(s) and the published article's title, journal citation, and DOI.

Trotterization is one of the simplest implementations, which has been extensively investigated theoretically [2, 12–17] and employed in various experiments such as in Refs. [6,9,11,18,19]. Despite recent developments, it may involve a huge number of gates when applied to a large-scale problem with over 50 qubits. For example, in Ref. [17] it has been estimated that we need 10^{15}–10^{18} gates to perform time evolution of simple molecules. Even for the simpler Heisenberg model, it is estimated that 10^{6}–10^{7} elementary rotation gates are needed [15]. These estimates are well beyond the reach of current quantum devices, the gate infidelities of which are on the order of 1%. Moreover, it is problematic even for an ideal fault-tolerant quantum computer because the execution of 10^{15} gates would require years even if it could perform 10^{8} gates per second.

It is therefore vital to develop methods that can compress the circuits for time evolution. The so-called qubitization technique [20] has achieved an optimal scaling in the number of gates needed. However, it requires ancilla qubits and a relatively large number of controlled gates and seems to be difficult in the NISQ era (see, e.g., Ref. [21]). When focusing on algorithms that require no or few ancilla qubits, Refs. [22,23], for example, have presented depth-compression methods for Trotter expansion based on some algebraic structures. Another promising approach is to use the framework of variational quantum algorithms [24–40]. These are exemplified by variational quantum simulation [25–33], and quantum compilations employing variational quantum diagonalization [34–36]. Among other methods, quantum-assisted quantum compiling (QAQC) [37,38] and its variant [39] comprise one of the promising ways to obtain approximate time-evolution operators with a compressed circuit depth. QAQC uses a variational quantum circuit V to approximate a target unitary U. Importantly, the authors have employed a local cost function instead of the naive global fidelity measure $\mathrm{Tr}(U^{\dagger}V)$ to avoid the barren-plateau problem. While QAQC is available for a generic target unitary gate U on L qubits, it seems to be problematic for depth compression that the target U itself should be accurately implemented on quantum circuits.

In this paper, we develop a local variational quantum compilation (LVQC) protocol to search an accurate and efficient quantum circuit for constructing large-scale local Hamiltonian dynamics with limited-size quantum devices or possibly with classical simulation of such limited-size quantum circuits. To formulate the protocol, we focus on the Lieb-Robinson (LR) bound [41], which dictates that the dynamics under a local Hamiltonian have approximate causal cones. We compose subsystem cost functions for every subsystem, which measure the local difference between the target unitary gate and the ansatz. Exploiting the LR bound, we rigorously derive scaling of the cost functions, which is validated when the subsystem size is as large as the approximate causal cone. These results lead

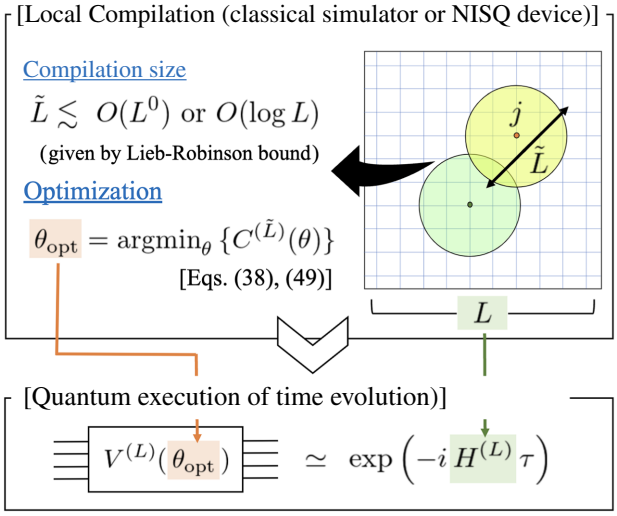

FIG. 1. An overview of the local variational quantum compilation (LVQC) protocol. We optimize the cost functions for the compilation size $\tilde{L}$, determined by the Lieb-Robinson (LR) bound. For finite-ranged and short-ranged interacting cases, this typically gives $\tilde{L} \lesssim O(L^0)$ or $\tilde{L} \lesssim O(\log L)$. We can directly implement a large-scale time-evolution operator with the optimal parameter θ_{opt}. LVQC can be completed by classical simulation with some approximation or NISQ devices, without implementing the target $\exp(-iH^{(L)}\tau)$ itself.

to our LVQC protocol as described in Fig. 1; we optimize a local-compilation cost function, corresponding to the average of the subsystem cost functions over the subsystems. This cost function can be computed with an at most $2\tilde{L}$-qubit quantum device or a corresponding classical simulator, where $\tilde{L}$ ($< L$ system size) denotes the scale of the causal-cone size. Finally, we construct a quantum circuit that approximates the target time-evolution operator for the system size L based on the resulting optimal parameters.

We also conduct a classical numerical demonstration of LVQC to compress the depth of the ideal time-evolution operators. We adopt a one-dimensional (1D) Heisenberg model and optimize the cost function for subsystems by approximately computing it with time-evolving block decimation (TEBD) [42,43]. We successfully compose a depth-5 time-evolution operator for 40 qubits by the local compilation for 20-qubit systems. This achieves an average gate fidelity of 0.9977, which is much better than that of the same-depth Trotterization, which is 0.8580. In addition, by computing the stroboscopic dynamics of ferromagnetic states with local excitations or domain walls, the optimal ansatz obtained by LVQC reproduces the dynamics with size and time scales twice and ten times as large as those used in the compilation, respectively.

We emphasize some advantages of LVQC. First, it requires at most $2\tilde{L}$-qubit quantum devices as large as the causal-cone size, which is comparably smaller than

the whole-system size L. There is no need to prepare the ideal target unitary gate for size L in our protocol. Second, our formulation relies only on the existence of the LR bounds. LVQC is available for broad systems involving finite-ranged, short-ranged, and long-ranged interactions in generic dimensions, with the help of the recent developments in the LR bound [44–52]. We expect that LVQC can be applied for executing large-scale time-evolution operators in the following ways:

(1) Classical local compilation with approximations *and* quantum execution in NISQ or larger systems.
(2) Quantum local compilation by NISQ devices *and* quantum execution in larger quantum devices.

The first case is exemplified by our numerical results based on TEBD. LVQC ensures the small-size compilation that is sometimes accessible with classical simulators employing some approximations. In that case, we can classically compile time-evolution operators without suffering noise and statistical errors and we can simulate large-scale quantum systems that are inaccessible only with classical simulators; long-time behavior beyond the coherence time will be observed in programmable quantum simulators by the optimized time-evolution operators. The second case is rather a long-term perspective. To simulate quantum materials with generic dimensions or interactions by NISQ devices or larger fault-tolerant quantum computers, the local-system size for the compilation will become at least hundreds or thousands of qubits. Such an intermediate scale required for LVQC will be just within the scope of NISQ devices in the near future and hence our results should contribute to bridging the gap between NISQ devices and larger-scale quantum computers.

The rest of this paper is organized as follows. In Sec. II, we introduce QAQC and the LR bound as the preliminaries for our results. We devote Secs. III, IV, and V to providing the main results. In Sec. III, we introduce the subsystem cost function, derived from the local cost functions of QAQC, and rigorously prove its scaling property by the LR bounds. In Sec. IV, we formulate the LVQC protocols for, respectively, translationally invariant systems and other generic systems. The above scaling yields the local compilation of large-scale Hamiltonian dynamics for both cases, while the protocol is simplified in the former case. Finally, we show its numerical verification in Sec. V and conclude this paper in Sec. VI.

II. PRELIMINARIES

In this section, we review some preliminary studies in order to derive our results on LVQC for large-scale Hamiltonian dynamics.

A. Quantum-assisted quantum compiling (QAQC)

QAQC [37] is a quantum-classical hybrid algorithm to obtain a variational quantum circuit $V(\theta)$ with parameters θ, which approximates a target unitary operator U. In Ref. [37], the authors have introduced several cost functions $C(U,V)$ that should be minimized to obtain an optimal parameter $\theta_{\rm opt}$ such that $U \simeq V(\theta_{\rm opt})$. The cost functions $C(U,V)$ should satisfy the following properties:

(1) (Computability) We can efficiently compute $C(U,V)$ with a quantum computer.
(2) (Faithfulness) $C(U,V)$ is always non-negative and it becomes zero if and only if U and V are equivalent.
(3) (Operational meaning) $C(U,V)$ provides constraints on some operationally meaningful value.

The first cost function is a global one, defined by

$$C_{\rm HST}(U,V) = 1 - \frac{1}{4^L}|{\rm Tr}[U^\dagger V]|^2, \tag{1}$$

where U and V are defined on an L-qubit lattice Λ. This can be measured by means of the Hilbert-Schmidt test (HST). In the HST, we use an $2L$-qubit lattice $\Lambda_A \cup \Lambda_B$ (each of Λ_A and Λ_B is a copy of Λ) and initialize the state by the Bell state $|\Phi_+\rangle_{AB}$, defined by

$$|\Phi_+\rangle_{AB} = \bigotimes_{j\in\Lambda} |\Phi_+\rangle_{A_jB_j}\,, \tag{2}$$

$$|\Phi_+\rangle_{A_jB_j} = \frac{1}{\sqrt{2}}(|00\rangle + |11\rangle)_{A_jB_j}\,. \tag{3}$$

The state $|\Phi_+\rangle_{A_jB_j}$ represents the Bell pair of the jth sites A_j and B_j, respectively, in Λ_A and Λ_B. Then, we apply U and V^*, respectively, to the subsystems A and B, resulting in the state

$$\rho_{AB}(U,V) = (U_A \otimes V_B^*)\,|\Phi_+\rangle_{AB}\,\langle\Phi_+|_{AB}\,(U_A\otimes V_B^*)^\dagger, \tag{4}$$

and perform the Bell measurements for every jth pair A_j and B_j. This is equivalent to measuring $\Pi_1\Pi_2\ldots\Pi_L$, where Π_j is defined by

$$\Pi_j = |\Phi_+\rangle_{A_jB_j}\,\langle\Phi_+|_{A_jB_j}\,. \tag{5}$$

Finally, since Eq. (1) can be rewritten as

$$C_{\rm HST}(U,V) = 1 - {\rm Tr}[\Pi_1\Pi_2\ldots\Pi_L\rho_{AB}(U,V)], \tag{6}$$

we can efficiently compute $C_{\rm HST}(U,V)$ with a $2L$-qubit quantum device. The term ${\rm Tr}[\Pi_1\Pi_2\ldots\Pi_L\rho_{AB}(U,V)]$ is schematically depicted in Fig. 2(a). The cost function $C_{\rm HST}(U,V)$ is faithful in that it satisfies $0 \le C_{\rm HST}(U,V) \le 1$

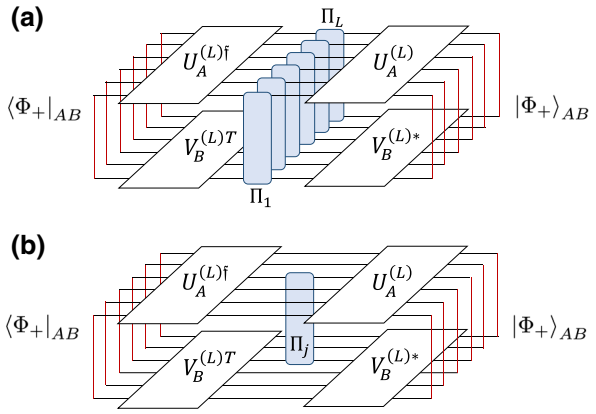

FIG. 2. A schematic picture of the way to compute the global and local cost functions. In each figure, the application of a Bell pair $|\Phi_+\rangle_{A_jB_j}$ indicates the taking of contractions on the jth pair A_j and B_j, which we represent by the red solid lines. (a) A schematic picture of $\mathrm{Tr}[\Pi_1 \ldots \Pi_L \rho_{AB}(U,V)]$, which gives the global cost function C_{HST} via Eq. (6). (b) A schematic picture of $\mathrm{Tr}[\Pi_j \rho_{AB}(U,V)]$, which gives the local cost function C_{LHST} via Eq. (8).

and in that it becomes zero if and only if there exists $\varphi \in \mathbb{R}$ such that $U = e^{i\varphi}V$.

The second cost function is local and is defined by

$$C_{\mathrm{LHST}}(U,V) = \frac{1}{L}\sum_{j=1}^{L} C_{\mathrm{LHST}}^{(j)}(U,V), \tag{7}$$

where each term is given by

$$C_{\mathrm{LHST}}^{(j)}(U,V) = 1 - \mathrm{Tr}[\Pi_j \rho_{\mathrm{AB}}(U,V)], \tag{8}$$

for $j = 1,2,\ldots,L$. They satisfy $0 \le C_{\mathrm{LHST}}(U,V) \le 1$ and $0 \le C_{\mathrm{LHST}}^{(j)}(U,V) \le 1$ by their definitions. We can compute them on a $2L$-qubit quantum device by means of the local Hilbert-Schmidt test (LHST), in which we perform Bell measurement of the jth pair, A_j and B_j, on the state $\rho_{AB}(U,V)$ for $C_{\mathrm{LHST}}^{(j)}(U,V)$ and take its average for $C_{\mathrm{LHST}}(U,V)$. The term $\mathrm{Tr}[\Pi_j \rho_{\mathrm{AB}}(U,V)]$ is described by Fig. 2(b). In terms of faithfulness, $C_{\mathrm{LHST}}^{(j)}(U,V)$ satisfies the following property:

$$\begin{aligned} &C_{\mathrm{LHST}}^{(j)}(U,V) = 0 \quad \text{if and only if} \\ &\quad {}^{\exists}\varphi \in \mathbb{R},\ {}^{\exists}W : \text{unitary, such that } UV^\dagger = e^{i\varphi} I_{\{j\}} \otimes W, \end{aligned} \tag{9}$$

where $I_{\{j\}}$ denotes the identity operator acting on the jth qubit. This indicates that the action of U corresponds to that of V on the jth site. Thus, the cost function $C_{\mathrm{LHST}}(U,V)$ becomes zero if and only if there exists $\varphi \in \mathbb{R}$ such that $U = e^{i\varphi}V$.

In the QAQC in Ref. [37], the authors employ either or the combined cost function

$$C_\alpha(U,V) = \alpha C_{\mathrm{HST}}(U,V) + (1-\alpha)C_{\mathrm{LHST}}(U,V), \tag{10}$$

with $0 \le \alpha \le 1$. It is faithful and it possesses an operational meaning in terms of the average gate fidelity, defined by

$$\bar{F}(U,V) = \int_\psi |\langle\psi|U^\dagger V|\psi\rangle|^2 d\psi, \tag{11}$$

where ψ is a Haar random state.

This indicates the expected fidelity between $U|\psi\rangle$ and $V|\psi\rangle$ averaged over a Haar random state $|\psi\rangle$ and it is bounded from below by the resulting cost functions as follows [37,53,54]:

$$\bar{F}(U,V) = 1 - \frac{2^{|\Lambda|}}{2^{|\Lambda|}+1} C_{\mathrm{HST}}(U,V), \tag{12}$$

$$\bar{F}(U,V) \ge 1 - \frac{2^{|\Lambda|}}{2^{|\Lambda|}+1} \cdot |\Lambda| C_{\mathrm{LHST}}(U,V), \tag{13}$$

where $|\Lambda|$ denotes the number of sites in the lattice Λ. The cost functions of QAQC can be efficiently computed on a $2L$-qubit quantum device based on Eqs. (6) and (8). As an alternative way to compute them, we prove the following lemma, which dictates that we can nontrivially reduce the resource for cost evaluation to L qubits (for the derivation, see Appendix A).

Lemma 1. $C_{\mathrm{HST}}(U,V)$ and $C_{\mathrm{LHST}}(U,V)$ for L-qubit unitaries U and V can be evaluated efficiently within an additive error ϵ with $\mathcal{O}(1/\epsilon^2)$ runs of an L-qubit device.

It should be noted that the algorithm to achieve Lemma 1 involves Monte Carlo sampling and induces an increased (though constant) overhead compared to the case where we use $2L$ qubits. In any cases, the bottleneck of QAQC for compressing time-evolution operators is to implement the target U itself on at least L-qubit quantum systems for cost evaluation. Our protocol can avoid this problem by compiling with smaller quantum systems with the size $\tilde{L}$, as large as the approximate causal cone by the LR bound, as discussed in Sec. IV,

B. Lieb-Robinson bound

The LR bound dictates that any local observable cannot spread out faster than a certain finite velocity (called the Lieb-Robinson velocity) under a local Hamiltonian [41]. This can be interpreted as the emergence of approximate causal cones in quantum mechanics.

Let us describe it more precisely. We focus on a local Hamiltonian on a lattice Λ, given by

$$H = \sum_{X \subseteq \Lambda} h_X, \tag{14}$$

where h_X denotes a term nontrivially acting on a domain $X \subseteq \Lambda$. Let $\|\cdot\|$ denote the operator norm. Here, we assume:

(1) (Extensiveness) The local energy scale at every site is bounded by a finite value g:

$$\sum_{X;X \ni j} \|h_X\| \leq g, \quad \text{for any} j \in \Lambda. \tag{15}$$

(2) (Locality of interactions) At most k-body interactions are involved with $k = O(1)$:

$$h_X = 0, \quad \text{if } |X| > k. \tag{16}$$

(3) (Range of interactions) Interactions are finite ranged with distance $d_H = O(1)$:

$$h_X = 0, \quad \text{if}^{\exists} j, j' \in X \text{ such that } \mathrm{dist}(j, j') > d_H. \tag{17}$$

Let us consider the local observables O_j and $O_{j'}$ acting on j and j', respectively, and assume that they are normalized as $\|O_j\| = \|O_{j'}\| = 1$. Then, the inequality

$$\|[U(\tau)^\dagger O_j U(\tau), O_{j'}]\| \leq C e^{-(\mathrm{dist}(j,j') - v\tau)/\xi}, \tag{18}$$

$$U(\tau) = e^{-iH\tau} \tag{19}$$

holds for a fixed time τ. Here, the constant velocity v and the constant length ξ are determined only by the extensiveness g, the locality k, and the range d_H, while the constant C depends additionally on τ (C typically increases linearly in τ [41]).

This suggests that $U(\tau)^\dagger O_j U(\tau)$ approximately acts on the domain inside the approximate causal cone $\{j' \in \Lambda \mid \mathrm{dist}(j, j') \leq v\tau\}$ and that the components outside of it are exponentially suppressed in the distance from j. As a result, it can be expected that $U(\tau)^\dagger O_j U(\tau)$ is well reproduced by the local Hamiltonian inside the approximate causal cone. Let $H^{(L',j)}$ denote the local Hamiltonian composed of h_X, the support X of which has distance from j smaller than $L'/2$ [for the exact definition, see Eqs. (23) and (24)]. In fact, we can derive the following inequality from the LR bound (see Ref. [50] and Appendix B):

$$\|U(\tau)^\dagger O_j U(\tau) - e^{iH^{(L',j)}\tau} O_j e^{-iH^{(L',j)}\tau}\| \leq \varepsilon_{\mathrm{LR}}, \tag{20}$$

$$\varepsilon_{\mathrm{LR}} = C' \int_{L'/2 - d_H}^{\infty} e^{-(x - v\tau)/\xi} dx = e^{-O(l_0/\xi)}, \tag{21}$$

where l_0 is defined by $L' = 2(l_0 + d_H + v\tau)$. The integration comes from the summation all over the lattice out of the approximate causal cone.

This relation enables us to approximate the local cost function (7) for a large size L by that for the smaller size L' with an arbitrarily small error $e^{-O(l_0/\xi)}$ when L' is sufficiently large compared to $v\tau$.

III. APPROXIMATION OF LOCAL COST FUNCTIONS BY LIEB-ROBINSON BOUND

In this section, we provide the first main result, where we compose the subsystem cost functions and show their scaling property by the LR bound. The subsystem cost functions are obtained by the restriction of systems to smaller subsystems for the local cost function C_{LHST}. We clarify the approximate causal cone from the LR bound and the exact causal cone from the ansatz in the local cost functions. They lead to two formulas, which are, respectively, raised as Propositions 2 and 3 below. As a result, we obtain how the error between the subsystem cost functions and C_{LHST} scales in the subsystem size $\tilde{L}$ and we validate the approximation of C_{LHST} by the subsystem cost functions with proper $\tilde{L}$. As we see in Sec. IV, these results enable the LVQC protocol for the whole-system Hamiltonian dynamics.

First, we specify the setup and the notation. We consider a local and extensive Hamiltonian with finite-ranged interactions, H, on a lattice Λ [see Eqs. (15)–(17)]. Throughout the main text, we focus on a 1D L-qubit system, as $\Lambda = \{1, 2, \ldots, L\}$, but the extension to other cases is straightforward (see Appendix B). We explicitly write the system size L like $H^{(L)}$ and consider the target time-evolution operator $U^{(L)} = \exp(-iH^{(L)}\tau)$. For simplicity, we employ a brickwork-structured ansatz, with the depth d in the form of

$$V^{(L)}(\theta) = \prod_{i=1}^{d} \left[\left(\prod_k V^{(2)}_{2k,2k+1}(\theta_{i,k}) \right) \left(\prod_k V^{(2)}_{2k-1,2k}(\theta'_{i,k}) \right) \right], \tag{22}$$

as described in Fig. 3. Here, $V^{(2)}_{j,j'}$ represents an arbitrary parametrized two-qubit gate on the neighboring sites j and j' and the parameter set θ is composed of $\{\theta_{i,k}\}_{i,k}$ and $\{\theta'_{i,k}\}_{i,k}$.

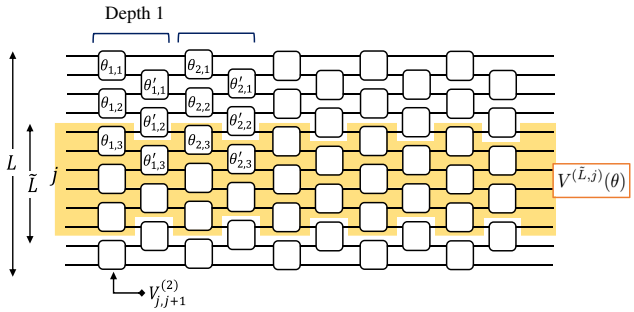

FIG. 3. The brickwork-structured ansatz $V^{(L)}(\theta)$, defined by Eq. (22). For translationally invariant systems, we choose the variational parameter set $\theta = \{\theta_{i,k}, \theta'_{i,k}\}_{i,k}$ so that $\theta_{i,k}$ and $\theta'_{i,k}$, respectively, become independent of the position k. The yellow region represents the j-centered $\tilde{L}$-size domain $\Lambda^{(\tilde{L},j)}$, which is utilized for the composition of the restricted ansatz $V^{(\tilde{L},j)}(\theta)$ based on Eq. (32).

Now, we derive two rigorous relations on the local cost function for each jth site, $C^{(j)}_{\mathrm{LHST}}(U^{(L)}, V^{(L)})$, using the approximate causal cone from the LR bound and the exact causal cone from the locality of the ansatz. The first of these, which is derived from the LR bound, validates the evaluation of the cost function with a local Hamiltonian acting only on qubits around the jth site. To be precise, when we define the j-centered L'-size domain $\Lambda^{(L',j)}$ and the restricted Hamiltonian $H^{(L',j)}$ by

$$\Lambda^{(L',j)} = \{j' \in \Lambda \,|\, |j - j'| \le L'/2\}, \tag{23}$$

$$H^{(L',j)} = \sum_{X; X \subseteq \Lambda^{(L',j)}} h_X, \tag{24}$$

for the L-qubit Hamiltonian $H^{(L)} = \sum_{X; X\subseteq\Lambda} h_X$, they are related to the local cost functions $C^{(j)}_{\mathrm{LHST}}(U^{(L)}, V^{(L)})$ by the following proposition.

Proposition 2. Let the restriction size L' be chosen by

$$L' = 2(l_0 + d_H + v\tau), \tag{25}$$

with a tunable parameter l_0, the range of the Hamiltonian d_H, and the LR velocity v. Then, the time-evolution operator under the restricted Hamiltonian, defined by

$$U^{(L',j)} = e^{-iH^{(L',j)}\tau} \otimes I_{\Lambda\setminus\Lambda_{L',j}}, \tag{26}$$

provides the following inequality:

$$C^{(j)}_{\mathrm{LHST}}(U^{(L)}, V^{(L)}) \le C^{(j)}_{\mathrm{LHST}}(U^{(L',j)}, V^{(L)}) + \frac{3}{4}\varepsilon_{\mathrm{LR}}. \tag{27}$$

Here, the term $\varepsilon_{\mathrm{LR}}$ is defined by Eqs. (20) and (21) and it is exponentially small in the tunable parameter l_0 as $\varepsilon_{\mathrm{LR}} = e^{-O(l_0/\xi)}$.

Proof. From the definition in Eq. (8), we obtain

$$\begin{aligned}
&|C^{(j)}_{\mathrm{LHST}}(U^{(L)}, V^{(L)}) - C^{(j)}_{\mathrm{LHST}}(U^{(L',j)}, V^{(L)})| \\
&\quad = |\mathrm{Tr}[\Pi_j \{\rho_{AB}(U^{(L)}, V^{(L)}) - \rho_{AB}(U^{(L',j)}, V^{(L)})\}]| \\
&\quad = |\,\langle\Phi_+|(U^{(L)}_A \otimes V^{(L)*}_B)^\dagger \Pi_j (U^{(L)}_A \otimes V^{(L)*}_B)|\Phi_+\rangle_{AB} \\
&\qquad - \langle\Phi_+|(U^{(L',j)}_A \otimes V^{(L)*}_B)^\dagger \Pi_j (U^{(L',j)}_A \otimes V^{(L)*}_B)|\Phi_+\rangle_{AB}\,|.
\end{aligned} \tag{28}$$

Considering that the projection to the Bell state is expanded by

$$\begin{aligned}
\Pi_j &= (|\Phi_+\rangle\langle\Phi_+|)_{A_jB_j} \\
&= \frac{1}{4}(I_{A_jB_j} + X_{A_j}X_{B_j} - Y_{A_j}Y_{B_j} + Z_{A_j}Z_{B_j}),
\end{aligned} \tag{29}$$

the right-hand side of Eq. (28) is bounded by

$$\begin{aligned}
&\frac{1}{4}\sum_{O=X,Y,Z} \|U^{(L)\dagger}_A O_{A_j} U^{(L)}_A - U^{(L',j)\dagger}_A O_{A_j} U^{(L',j)}_A\| \\
&\qquad \times \|V^{(L)\mathrm{T}}_B O_{B_j} V^{(L)*}_B\|\,\langle\Phi_+|\Phi_+\rangle_{AB} \\
&\quad \le \frac{3}{4}\varepsilon_{\mathrm{LR}}.
\end{aligned} \tag{30}$$

The above inequality comes from Eq. (20), the LR bound for the local observable. Finally, we obtain the relation

$$|C^{(j)}_{\mathrm{LHST}}(U^{(L)}, V^{(L)}) - C^{(j)}_{\mathrm{LHST}}(U^{(L',j)}, V^{(L)})| \le \frac{3}{4}\varepsilon_{\mathrm{LR}}, \tag{31}$$

which implies the inequality given in Eq. (27). ■

This proposition says that the restriction of the Hamiltonian to a smaller region hardly alters the local cost functions. The difference is bounded by the LR bound error $\varepsilon_{\mathrm{LR}}$. Equivalently, the diagram of Fig. 2(b), which gives C_{LHST}, can be approximated by that of Fig. 4(a), which gives the restricted version. We note that this proof relies only on the existence of the LR bound and hence Proposition 2 is also valid for generic locally interacting systems in any dimension. For 1D systems with finite-ranged interactions, we have $\varepsilon_{\mathrm{LR}} = \exp(-O(l_0/\xi))$ with $L' = 2(l_0 + d_H + v\tau)$ from Eq. (21). Based on this proposition, we can accurately determine the upper bound of the local cost function $C^{(j)}_{\mathrm{LHST}}(U^{(L)}, V^{(L)})$ by evaluating $C^{(j)}_{\mathrm{LHST}}(U^{(L',j)}, V^{(L)})$.

At this stage, however, measurement of the cost functions requires $2L$-qubit quantum devices or L-qubit quantum devices with sampling due to the existence of $V^{(L)}$. To overcome this obstacle, we employ causal cones of the ansatz $V^{(L)}$ and show that $C^{(j)}_{\mathrm{LHST}}(U^{(L',j)}, V^{(L)})$ can be evaluated with smaller-size quantum devices without any

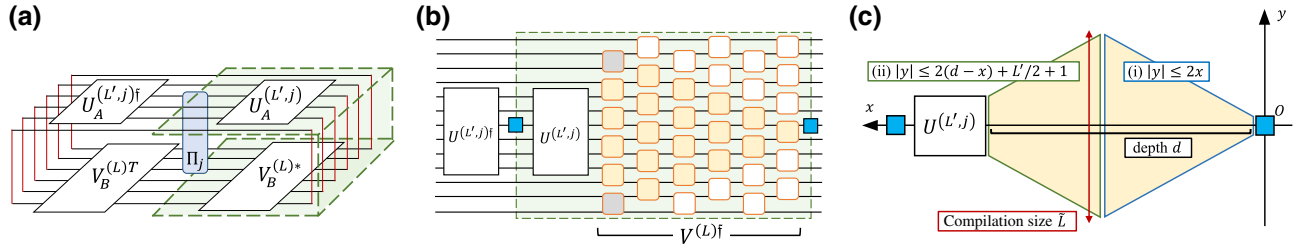

FIG. 4. (a) A diagrammatic description of $\mathrm{Tr}(\Pi_j \rho_{AB}(U^{(L',j)}, V^{(L)}))$. This gives an approximate upper bound of the local cost function $C^{(j)}_{\mathrm{LHST}}(U^{(L)}, V^{(L)})$ via Proposition 2. (b) Part of the gates composing $\mathrm{Tr}(\Pi_j \rho_{AB}(U^{(L',j)}, V^{(L)}))$, designated by the green region in (a). Only the orange two-qubit gates in $V^{(L)\dagger}$ are active, while the other gray and white two-qubit gates vanish due to their positions being out of the causal cones. (c) A schematic picture of the active region in the ansatz $V^{(L)}$. All the active two-qubit gates are included in the yellow domain. Its height determines the proper compilation size $\tilde{L}$.

approximation. For the j-centered $\tilde{L}$-site domain $\Lambda_{\tilde{L},j}$, let us define a restricted ansatz $V^{(\tilde{L},j)}(\theta)$ by

$$V^{(\tilde{L},j)}(\theta) = \prod_{i=1}^{d}\left[\left(\prod_{k}^{(\tilde{L},j)} V^{(2)}_{2k,2k+1}(\theta_{i,k})\right)\left(\prod_{k}^{(\tilde{L},j)} V^{(2)}_{2k-1,2k}(\theta'_{i,k})\right)\right], \tag{32}$$

from the depth-d ansatz $V^{(L)}(\theta)$ of Eq. (22). Here, the symbols $\Pi_k^{(\tilde{L},j)}$ represent the product over k such that the support of $V^{(2)}_{2k,2k+1}(\theta_{i,k})$ (for the first one) or $V^{(2)}_{2k-1,2k}(\theta_{i,k})$ (for the second one) is included in the domain $\Lambda_{\tilde{L},j}$ (see Fig. 3). Then, we obtain the following proposition.

Proposition 3. We consider the same situation as that of Proposition 2. We assume $4d \ge L'$ for the depth-d L-site ansatz $V^{(L)}(\theta)$, and rewrite the depth as $d = L'/4 + d'$ ($d' \ge 0$ is chosen so that d becomes an integer). For $\tilde{L}$ satisfying $\tilde{L} \ge L' + 2d' + 1$, where the right-hand side represents the size of the approximate causal cones, the depth-d $\tilde{L}$-site ansatz $V^{(\tilde{L},j)}(\theta)$ satisfies the following equality:

$$C^{(j)}_{\mathrm{LHST}}(U^{(L',j)}, V^{(L)}) = C^{(j)}_{\mathrm{LHST}}(\tilde{U}^{(L',j)}, V^{(\tilde{L},j)}). \tag{33}$$

Here, $\tilde{U}^{(L',j)}$ represents the restriction of $U^{(L',j)}$ to the domain $\Lambda_{\tilde{L},j}$, which is given by

$$\tilde{U}^{(L',j)} = e^{-iH^{(L',j)}\tau} \otimes I_{\Lambda_{\tilde{L},j}\setminus\Lambda_{L',j}}. \tag{34}$$

Remark.—The assumption $4d \ge L'$ is not essentially required to prove this proposition. Rather, it serves as a guideline to construct the ansatz $V^{(L)}$. When we employ the brickwork-structured ansatz given by Eq. (22), a local observable acting on a single qubit generally spreads to $4d$-qubit operators. Hence, we should use d such that $4d \ge L'$ to capture the correlation within the LR bound and thereby accurately approximate the time evolution. It is straightforward to generalize the above proposition to smaller d with a slight modification of $\tilde{L}$.

Proof. We employ the causal cones of quantum circuits here. Let us focus on $\mathrm{Tr}[\Pi_j \rho_{AB}(U^{L',j}, V^{(L)})]$, which can be schematically depicted by Fig. 4(a). To visualize the causal cone, we pick up a part of the circuit belonging to the right half in the figure (the light-green region), which results in Fig. 4(b). The light-blue squares in Fig. 4(b) represent local operators on j th sites composing Π_j, given by Eq. (29). We also note that $V_B^{(L)*}$ in Fig. 4(a) is translated into $V^{(L)\dagger}$, since its input and output are exchanged.

Each local two-qubit gate in the ansatz $V^{(L)\dagger}$ can be classified into one of three groups by its effect on the local cost function. The first group is depicted by the white (non-painted) two-qubit gates in Fig. 4(b). Since these local gates and the corresponding ones in $V_B^{(L)\mathrm{T}}$ cancel each other by the contraction in the lower layer of Fig. 4(a), they do not affect $\mathrm{Tr}[\Pi_j \rho_{AB}(U^{(L',j)}, V^{(L)})]$. This cancellation is due to the locality of Π_j and is independent of $U_A^{(L',j)}$ appearing in the upper layer. The second group, composed of the gray two-qubit gates, are also inactive, because they can be contracted to identity in the upper layer. In contrast to the first group, its cancellation originates from the size restriction of the Hamiltonian $H^{(L)}$ to $H^{(L')}$, validated by the LR bound. The last group is composed of the yellow gates residing within the causal cones. Only these two-qubit gates are relevant for $\mathrm{Tr}[\Pi_j \rho_{AB}(U^{(L',j)}, V^{(L)})]$, which can be schematically depicted as Fig. 4(c).

Finally, we determine the proper compilation size $\tilde{L}$. The active region, composed of the two causal cones spreading from the left and the right side [see (i) and (ii) in Fig. 4(c)], is designated by

$$|y| \le \min\{2(d-x) + L'/2 + 1, 2x\}, \quad 0 \le x \le d. \tag{35}$$

When the compilation size $\tilde{L}$ surpasses its height, that is, when

$$\tilde{L} \geq \frac{L'}{2} + 2d + 1 = L' + 2d' + 1, \tag{36}$$

the restricted ansatz $V^{(\tilde{L},j)}(\theta)$ includes all the two-qubit gates in the active region. Therefore, we have

$$\begin{aligned}
&\mathrm{Tr}[\Pi_j \rho_{AB}(U^{(L',j)}, V^{(L)})] \\
&\quad = \mathrm{Tr}[\Pi_j \rho_{AB}(e^{-iH^{(L',j)}\tau} \otimes I_{\Lambda\setminus\Lambda_{L',j}}, V^{(\tilde{L},j)} \otimes I_{\Lambda\setminus\Lambda_{\tilde{L},j}})] \\
&\quad = \mathrm{Tr}[\Pi_j \rho_{AB}(e^{-iH^{(L',j)}\tau} \otimes I_{\Lambda_{\tilde{L},j}\setminus\Lambda_{L',j}}, V^{(\tilde{L},j)})],
\end{aligned} \tag{37}$$

where we use the fact that the contraction over $\Lambda\setminus\Lambda_{\tilde{L},j}$ gives identity for the last equality. By using the definitions of the local cost function $C^{(j)}_{\mathrm{LHST}}$ and the restricted time evolution $\tilde{U}^{(L',j)}$ [see Eqs. (8) and (34), respectively], we complete the proof of Proposition 3. ■

Let us define the subsystem cost function by $C^{(j)}_{\mathrm{LHST}}(\tilde{U}^{(L',j)}, V^{(\tilde{L},j)})$, which can be measured by a $2\tilde{L}$-qubit quantum device or a $\tilde{L}$-qubit quantum device with Monte Carlo sampling based on Lemma 1. Propositions 2 and 3 yield that the local cost function $C^{(j)}_{\mathrm{LHST}}(U^{(L)}, V^{(L)})$ can be approximated by the subsystem cost function and they also dictate the scaling property of the subsystem cost function in the subsystem size $\tilde{L}$. Importantly, $\tilde{L} \geq L' + 2d' + 1 = 2(l_0 + d_H + v\tau) + 2d' + 1$ can be independent of the whole-system size L and significantly smaller than L. We note that the coefficient of the depth d in $\tilde{L}$ comes from the brickwork structure of the ansatz $V^{(L)}$. We can obtain the same result for any other ansatz by changing the coefficient in $\tilde{L}$ as long as it is local.

IV. LOCAL VARIATIONAL QUANTUM COMPILATION OF A LARGE-SCALE HAMILTONIAN DYNAMICS

In this section, we formulate the LVQC of large-scale Hamiltonian dynamics as the second main result. In our protocol, we construct an approximate time-evolution operator for the large size L by optimizing the cost functions defined on the smaller size $\tilde{L}$. Based on Propositions 2 and 3, we provide two different formulations for translationally invariant cases (Sec. IV A) and generic cases (Sec. IV B).

A. Local compilation for translationally invariant systems

We first deal with translationally invariant cases under periodic boundary conditions (PBC). Throughout this section, we denote such a translationally invariant Hamiltonian and its time-evolution operator for the size L as $H^{(L)}_{\mathrm{PBC}}$ and $U^{(L)}_{\mathrm{PBC}}$. Then, it is reasonable also to impose translation invariance and PBC on the ansatz, denoted by $V^{(L)}_{\mathrm{PBC}}$. To be precise, we assume that the variational parameter set $\theta = \{\theta_{i,k}, \theta'_{i,k}\}_{i,k}$ is independent of the position k. The number of parameters in $V^{(L)}_{\mathrm{PBC}}(\theta)$ depends only on the depth d. Based on Propositions 2 and 3, we can derive the following theorem, which also shows the protocol of LVQC.

Theorem 4. We define the local-compilation cost function by

$$\begin{aligned}
C^{(\tilde{L})}_{\alpha}(\theta) = \alpha C_{\mathrm{HST}}(U^{(\tilde{L})}_{\mathrm{PBC}}, V^{(\tilde{L})}_{\mathrm{PBC}}(\theta)) \\
+ (1-\alpha) C_{\mathrm{LHST}}(U^{(\tilde{L})}_{\mathrm{PBC}}, V^{(\tilde{L})}_{\mathrm{PBC}}(\theta)),
\end{aligned} \tag{38}$$

for a certain $\alpha \in [0,1]$, which is defined on an $\tilde{L}$-size translationally invariant systems under PBC. Assume that, after the minimization of $C^{(\tilde{L})}_{\alpha}(\theta)$, the optimal parameter set θ_{opt} gives the upper bound of the local and global cost functions as

$$C_{\mathrm{LHST}}(U^{(\tilde{L})}_{\mathrm{PBC}}, V^{(\tilde{L})}_{\mathrm{PBC}}(\theta_{\mathrm{opt}})) < \varepsilon_{\mathrm{LHST}}, \tag{39}$$

$$C_{\mathrm{HST}}(U^{(\tilde{L})}_{\mathrm{PBC}}, V^{(\tilde{L})}_{\mathrm{PBC}}(\theta_{\mathrm{opt}})) < \varepsilon_{\mathrm{HST}}. \tag{40}$$

When we choose the smallest even number larger than $2(l_0 + d_H + v\tau) + 2d' + 1$ as the compilation size $\tilde{L}$, the time-evolution operator for an L-qubit system ($L \geq \tilde{L}$) is approximated as

$$C_{\mathrm{LHST}}(U^{(L)}_{\mathrm{PBC}}, V^{(L)}_{\mathrm{PBC}}(\theta_{\mathrm{opt}})) \leq \varepsilon_{\mathrm{LHST}} + \frac{3}{2}\varepsilon_{\mathrm{LR}}, \tag{41}$$

$$C_{\mathrm{HST}}(U^{(L)}_{\mathrm{PBC}}, V^{(L)}_{\mathrm{PBC}}(\theta_{\mathrm{opt}})) \leq L\left(\varepsilon_{\mathrm{HST}} + \frac{3}{2}\varepsilon_{\mathrm{LR}}\right), \tag{42}$$

with the usage of the same parameter set θ_{opt}.

Proof. We first derive Eq. (41) from Eq. (39). We combine translation symmetry with the scaling property of the subsystem cost functions, represented by Propositions 2 and 3. As a result, we obtain the relation for any j,

$$\begin{aligned}
C_{\mathrm{LHST}}(U^{(L)}_{\mathrm{PBC}}, V^{(L)}_{\mathrm{PBC}}) &= C^{(j)}_{\mathrm{LHST}}(U^{(L)}_{\mathrm{PBC}}, V^{(L)}_{\mathrm{PBC}}) \\
&\leq C^{(j)}_{\mathrm{LHST}}(\tilde{U}^{(L',j)}, V^{(\tilde{L},j)}) + \frac{3}{4}\varepsilon_{\mathrm{LR}}.
\end{aligned} \tag{43}$$

Here, $\tilde{U}^{(L',j)}$ and $V^{(\tilde{L},j)}$ are constructed from $U^{(L)}_{\mathrm{PBC}}$ and $V^{(L)}_{\mathrm{PBC}}$ by the restriction to L'- and $\tilde{L}$-size systems, respectively [see Eqs. (34) and (32)]. They have open boundary conditions (OBCs) as illustrated in Fig. 5 and therefore do not straightforwardly relate to $U^{(\tilde{L})}_{\mathrm{PBC}}$ and $V^{(\tilde{L})}_{\mathrm{PBC}}$. To

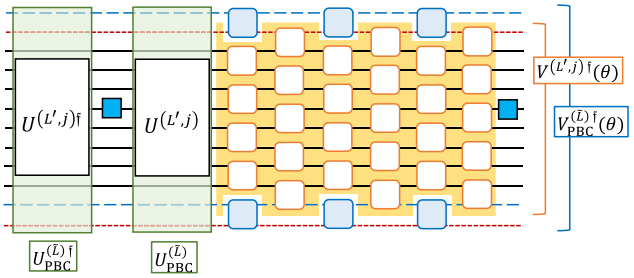

FIG. 5. A schematic version of Fig. 4(b) for translationally invariant systems under PBC. The blue and red solid lines, respectively, represent identical sites.

recover the PBC, we adopt the following strategy. Figure 5 gives a schematic picture of part of the gates composing $\mathrm{Tr}[\Pi_j \rho_{AB}(\tilde{U}^{L',j}, V^{(\tilde{L},j)})]$, similar to Fig. 4(b). First, we add two-qubit gates $V^{(2)}_{\tilde{L},1}$ to each layer of the restricted ansatz $V^{(\tilde{L},j)}$, represented by the light-blue squares at the boundaries in Fig. 5. When the parameter set of each $V^{(2)}_{\tilde{L},1}$ is the same as that of the two-qubit gate in the same layer, it reproduces the translationally invariant ansatz under PBC, $V^{(\tilde{L})}_{\mathrm{PBC}}$. Since local gates outside of the causal cones do not alter the local cost function at all, we obtain the following relation:

$$C_{\mathrm{LHST}}(U^{(L)}_{\mathrm{PBC}}, V^{(L)}_{\mathrm{PBC}}) \le C^{(j)}_{\mathrm{LHST}}(\tilde{U}^{(L',j)}, V^{(\tilde{L})}_{\mathrm{PBC}}) + \frac{3}{4}\varepsilon_{\mathrm{LR}}. \quad (44)$$

We also recover the PBC of the target unitary $\tilde{U}^{(L',j)}$. Let us consider the two Hamiltonians $H^{(\tilde{L})}_{\mathrm{PBC}}$ and $H^{(L',j)}$, which, respectively, provide the time-evolution operators $U^{(\tilde{L})}_{\mathrm{PBC}}$ and $\tilde{U}^{(L',j)}$. Since the Hamiltonian $H^{(L',j)}$ becomes the restriction of $H^{(\tilde{L})}_{\mathrm{PBC}}$ from the domain $\Lambda_{\tilde{L},j}$ to the one denoted by $\Lambda_{L',j}$, we can again employ the inequality Eq. (20) generated by the LR bound,

$$\| U^{(\tilde{L})\dagger}_{\mathrm{PBC}} O_j U^{(\tilde{L})}_{\mathrm{PBC}} - \tilde{U}^{(L',j)\dagger} O_j \tilde{U}^{(L',j)} \| \le \varepsilon_{\mathrm{LR}}, \quad (45)$$

for any local normalized observable at a jth site, O_j. This implies that we can apply Propositions 2 and 3 by substituting $U^{(\tilde{L})}_{\mathrm{PBC}}$ for $U^{(L)}$, which results in

$$C^{(j)}_{\mathrm{LHST}}(\tilde{U}^{(L',j)}, V^{(\tilde{L})}_{\mathrm{PBC}}) \le C^{(j)}_{\mathrm{LHST}}(U^{(\tilde{L})}_{\mathrm{PBC}}, V^{(\tilde{L})}_{\mathrm{PBC}}) + \frac{3}{4}\varepsilon_{\mathrm{LR}} < \varepsilon_{\mathrm{LHST}} + \frac{3}{4}\varepsilon_{\mathrm{LR}}. \quad (46)$$

Combining this inequality with Eq. (44), we arrive at the relation of C_{LHST}, given by Eq. (41).

Next, we derive Eq. (42), which gives an upper bound of the global cost function C_{HST}. We employ the following inequality [37]:

$$C_{\mathrm{LHST}}(U, V) \le C_{\mathrm{HST}}(U, V) \le |\Lambda| C_{\mathrm{LHST}}(U, V), \quad (47)$$

where two unitary gates, U and V, are defined on a lattice Λ. Under the assumption of Eq. (40), we have $C_{\mathrm{LHST}}(U^{(\tilde{L})}_{\mathrm{PBC}}, V^{(\tilde{L})}_{\mathrm{PBC}}(\theta_{\mathrm{opt}})) < \varepsilon_{\mathrm{HST}}$ from the first inequality in Eq. (47). Using the above result for the local cost function C_{LHST}, Eq. (41), we obtain $C_{\mathrm{LHST}}(U^{(L)}_{\mathrm{PBC}}, V^{(L)}_{\mathrm{PBC}}(\theta_{\mathrm{opt}})) \le \varepsilon_{\mathrm{HST}} + \frac{3}{2}\varepsilon_{\mathrm{LR}}$. Finally, considering $|\Lambda| = L$ for a 1D system, the second inequality in Eq. (47) implies Eq. (42). ■

This theorem tells us that the optimal parameter set θ_{opt} for the $\tilde{L}$-size local-compilation cost function can be directly employed to construct the approximate larger-scale time evolution by $U^{(L)}_{\mathrm{PBC}} \simeq V^{(L)}_{\mathrm{PBC}}(\theta_{\mathrm{opt}})$. Its accuracy can be guaranteed by Eq. (41) or Eq. (42). The error consists of two parts: the first terms, $\varepsilon_{\mathrm{LHST}}$ and $\varepsilon_{\mathrm{HST}}$, are due to a limited expressive power of the ansatz $V^{(\tilde{L})}_{\mathrm{PBC}}$; the second term, $\varepsilon_{\mathrm{LR}}$, is the intrinsic error induced by this LVQC protocol. They can be improved by using more expressive ansatz and using a larger compilation size $\tilde{L}$, respectively.

Now, we discuss what compilation size should be used to achieve an accuracy of $O(\varepsilon)$ for a quantity of interest. When we focus on some local observables under the approximate time evolution $V^{(L)}_{\mathrm{PBC}}(\theta_{\mathrm{opt}})$, the local cost function C_{LHST} plays a significant role, since it guarantees the local equivalence with $U^{(L)}_{\mathrm{PBC}}$ by Eq. (9). To be more precise, $C_{\mathrm{LHST}} = O(\varepsilon)$ implies additive error $O(\varepsilon)$ in the expectation values of the local observables. We wish to choose the compilation size $\tilde{L} = 2\lceil l_0 + d_H + v\tau + d' + 1/2\rceil$ so that $\varepsilon_{\mathrm{LR}} = e^{-O(l_0/\xi)}$ can be neglected. Therefore, in this case, $\tilde{L}$ can be taken as $O(\xi \log(1/\epsilon)) + 2d_H + 2v\tau + 2d'$, which is independent of the whole-system size L.

On the other hand, in the cases where we require the accuracy in terms of global observables, the average gate fidelity $\bar{F}$ has operational meaning. $1 - \bar{F} = O(\varepsilon)$ implies an accuracy of $O(\varepsilon)$ in the expectation values of any observables. When the $\tilde{L}$-size optimization is achieved as in Eqs. (39) and (40), the combination with Eq. (12) or Eq. (13) ensures its lower bound as

$$\bar{F}(U^{(L)}_{\mathrm{PBC}}, V^{(L)}_{\mathrm{PBC}}(\theta_{\mathrm{opt}})) \ge 1 - \frac{2^{|\Lambda|}}{2^{|\Lambda|}+1} \times L\left(\varepsilon_{\mathrm{LHST}} + \frac{3}{2}\varepsilon_{\mathrm{LR}}\right) \ge 1 - \frac{2^{|\Lambda|}}{2^{|\Lambda|}+1} \times L\left(\varepsilon_{\mathrm{HST}} + \frac{3}{2}\varepsilon_{\mathrm{LR}}\right). \quad (48)$$

Therefore, to achieve $1 - \bar{F} = O(\varepsilon)$, we should choose the compilation size $\tilde{L}$ satisfying $L\varepsilon_{\mathrm{LR}} = e^{-O(l_0/\xi)+\log L} = O(\varepsilon)$, which results in $\tilde{L} = O(\xi \log(1/\varepsilon) + \xi \log L) + 2d_H + 2v\tau + 2d'$. Upon this choice of the compilation size, we should continue the optimization of $C^{(\tilde{L})}_{\alpha}(\theta)$ until $\varepsilon_{\mathrm{LHST}}$ or $\varepsilon_{\mathrm{HST}}$ becomes much smaller than $O(L^{-1})$ and then we can obtain the preferred accuracy.

Let us discuss the feasibility of the local optimization, given by Eqs. (39) and (40). The form of the cost function is quite similar to that of QAQC and hence we can adopt various strategies for the optimization; either a gradient-based or a gradient-free parameter update is available [37]. Not only does reduction in the compilation size make optimization easier compared to other variational methods such as QAQC but also it sometimes enables classical optimization free from statistical errors, as numerically demonstrated in Sec. V. In addition, even when the variational parameters fail to converge or find the optimal solution, the compression will be successful to some extent. Theorem 4 itself is valid for arbitrary parameters θ from the derivation. Therefore, by starting the optimization with a certain good choice of the known initial ansatz, we can improve its efficiency if several parameter updates achieve the lower cost function. For instance, as discussed in Sec. V, we can compose the ansatz so that it includes the Trotterization. By setting the initial ansatz to the Trotterization, it is expected that we can almost always find more efficient implementation compared to Trotterization.

To summarize, our protocol starts with choosing a proper compilation size $\tilde{L}$. $\tilde{L}$ should taken to be comparable to the approximate causal-cone size by the LR bound, $2(\xi + d_H + v\tau + d')$, or a bit larger than it, depending on the desired error. After minimizing the local-compilation cost function $C_\alpha^{(\tilde{L})}(\theta)$, which can be evaluated using a classical simulator or a quantum device with at least $\tilde{L}$ qubits, we can directly apply the optimal parameter set $\theta_{\rm opt}$ to obtain the approximate time evolution $U_{\rm PBC}^{(L)} \simeq V_{\rm PBC}^{(L)}(\theta_{\rm opt})$. This reduction in the size makes NISQ devices or classical simulators employing some approximation (see Sec. V) suitable for the compilation. LVQC can be employed for various purposes, such as depth compression and calibration of $U^{(L)}$, without implementing the target $U^{(L)}$ itself. In other words, it is sufficient to prepare $U^{(\tilde{L})}$, which is the time-evolution for smaller systems. This is clearly one of the principal advantages of our protocol. We summarize the results in Fig. 1.

B. Local compilation for generic systems without translation invariance

Here, we develop the LVQC protocol for 1D finite-ranged systems without translation invariance. The result is not essentially altered from the translationally invariant cases but they have different cost functions.

We directly use Propositions 2 and 3 to derive the protocol. For the brickwork-structured ansatz $V^{(L)}(\theta)$ (not necessarily translationally invariant), we define the local-compilation cost function for generic cases by

$$C^{(\tilde{L})}(\theta) = \frac{1}{L}\sum_{j=1}^{L} C_{\rm LHST}^{(j)}(\tilde{U}^{(L',j)}, V^{(\tilde{L},j)}(\theta)), \tag{49}$$

where we directly use the subsystem cost functions $C_{\rm LHST}^{(j)}(\tilde{U}^{(L',j)}, V^{(\tilde{L},j)}(\theta))$. With the help of Propositions 2 and 3, we immediately obtain

$$\begin{aligned} &|C_{\rm LHST}(U^{(L)}, V^{(L)}) - C^{(\tilde{L})}(\theta)| \\ &\le \frac{1}{L}\sum_{j=1}^{L} |C_{\rm LHST}^{(j)}(U^{(L)}, V^{(L)}) - C_{\rm LHST}^{(j)}(\tilde{U}^{(L',j)}, V^{(\tilde{L},j)})| \\ &\le \frac{3}{4}\varepsilon_{\rm LR}. \end{aligned} \tag{50}$$

We also use the relation given in Eq. (47), which results in

$$C_{\rm HST}(U^{(L)}, V^{(L)}) \le L\left(C^{(\tilde{L})}(\theta) + \frac{3}{4}\varepsilon_{\rm LR}\right). \tag{51}$$

Therefore, we obtain the following theorem, which designates the protocol for generic cases.

Theorem 5. We variationally minimize the local-compilation cost function $C^{(\tilde{L})}(\theta)$. When the optimal parameter set $\theta_{\rm opt}$ gives $C^{(\tilde{L})}(\theta_{\rm opt}) \le \varepsilon_{\rm LHST}$, the cost functions for the size L are bounded by

$$C_{\rm LHST}(U^{(L)}, V^{(L)}(\theta_{\rm opt})) \le \varepsilon_{\rm LHST} + \frac{3}{4}\varepsilon_{\rm LR}, \tag{52}$$

$$C_{\rm HST}(U^{(L)}, V^{(L)}(\theta_{\rm opt})) \le L\left(\varepsilon_{\rm LHST} + \frac{3}{4}\varepsilon_{\rm LR}\right). \tag{53}$$

The average gate fidelity is bounded from below as follows:

$$\bar{F}(U^{(L)}, V^{(L)}(\theta_{\rm opt})) \ge 1 - \frac{2^{|\Lambda|}}{2^{|\Lambda|+1}} \times L\left(\varepsilon_{\rm LHST} + \frac{3}{4}\varepsilon_{\rm LR}\right). \tag{54}$$

Based upon this theorem, we can perform the local compilation in a similar way to translationally invariant systems, while the cost function is replaced by Eq. (49). We have the same compilation size $\tilde{L} = 2\lceil l_0 + d_H + v\tau + d' + 1/2\rceil$ with l_0 such that $\varepsilon_{\rm LR}$ or $L\varepsilon_{\rm LR}$ becomes sufficiently small. After the local optimization that achieves $\varepsilon_{\rm LHST} \ll 1$ or $L\varepsilon_{\rm LHST} \ll 1$, we use the optimal parameter set $\theta_{\rm opt}$ for the L-size time-evolution operator as schematically shown in Fig. 1.

We also remark on an extension of our protocol to other generic cases. Our protocol relies only on the existence of the LR bound, given by Eq. (20), and the locality of the ansatz. Thus, the extension to higher-dimensional systems, in which we change the form of $\varepsilon_{\rm LR}$ and replace the coefficient L in Eqs. (42) or (53) by $|\Lambda| \sim L^D$, is straightforward. We can also consider short-ranged or long-ranged interactions since they, respectively, show an exponential or polynomial decay of the error $\varepsilon_{\rm LR}$ (Note that we require

additional conditions when considering long-ranged interactions for the existence of the LR bound, as discussed in Appendix B 4.) The compilation size $\tilde{L}$ increases at most in $O(\log L)$ (for finite-ranged and short-ranged interactions in generic dimensions) or in $O(L^\sigma)$ with $\sigma < 1$ (long-ranged interactions in generic dimensions). We can expect a significant reduction in the compilation size for a broad class of locally interacting systems to compile large-scale time-evolution operators. For a detailed discussion, see Appendix B.

C. Efficient computation of long-time-scale dynamics

In our compilation protocol, we optimize the time evolution for a certain fixed time τ. By repeatedly applying the compressed time evolution $V^{(L)}(\theta_{\rm opt})$, we can also efficiently simulate the longer-time-scale stroboscopic dynamics at $t = n\tau$ ($n \in \mathbb{N}$).

Let us evaluate the error when we compute the longer time scale with the compressed gates $V^{(L)}(\theta_{\rm opt})$. By using the relation $\|U^n - V^n\|_F \le n\|U - V\|_F$ for the Frobenius norm $\|\cdot\|_F$, the global cost function $C_{\rm HST}$ satisfies the following inequality [34]:

$$C_{\rm HST}(U^n, V^n) \lesssim n^2 C_{\rm HST}(U, V), \tag{55}$$

where the condition $n^2 C_{\rm HST}(U, V) \ll 1$ is supposed. When we optimize the local-compilation cost function and obtain $C^{(\tilde{L})}(\theta_{\rm opt}) \le \varepsilon_{\rm LHST}$ based on Theorem 5, the resulting cost function for size L and time $t = n\tau$ is bounded by

$$C_{\rm HST}(U^{(L)}(n\tau), [V^{(L)}(\theta_{\rm opt})]^n) \lesssim Ln^2\left(\varepsilon_{\rm LHST} + \frac{3}{4}\varepsilon_{\rm LR}\right). \tag{56}$$

To make it much smaller than 1, we slightly modify the protocol. First, we choose the compilation size $\tilde{L}$ so that $Ln^2\varepsilon_{\rm LR}$ becomes negligible. The typical scale of $\tilde{L}$ is given by

$$\tilde{L} \gtrsim 2(\xi + d_H + v\tau) + \xi \log L + 2\xi \log n, \tag{57}$$

by Eq. (21). Then, the local optimization of $C^{(\tilde{L})}(\theta)$ should be continued until $Ln^2\varepsilon_{\rm LHST} \ll 1$ is achieved. We note that the compilation size $\tilde{L}$ is hardly affected by the time of interest, $t = n\tau$, as it increases in proportion to $\log n$.

V. NUMERICAL DEMONSTRATION OF DEPTH COMPRESSION

Here, we numerically demonstrate LVQC and, in particular, we try to compress the depth of a large-scale time-evolution operator by the compilation. For simplicity, we concentrate on 1D systems and rely on classical simulation by TEBD, based on matrix product states (MPSs) [42,43,55,56].

We first introduce the model and the ansatz. We adopt an antiferromagnetic (AFM) Heisenberg model on a 1D lattice, defined by

$$H^{(L)}_{\rm AFM} = \sum_{j=1}^{L-1}(X_jX_{j+1} + Y_jY_{j+1} + Z_jZ_{j+1}). \tag{58}$$

We employ OBC to make it easier to simulate by MPS. The target of the depth compression is the time-evolution operator $U^{(L)} = \exp(-iH^{(L)}_{\rm AFM}\tau)$ with a fixed time τ. On the other hand, we give the ansatz $V^{(L)}(\theta)$ by the brickwork-structured circuit under OBC, designated by Eq. (22). We parametrize each of two-qubit gates in it by

$$V^{(2)}_{j,j+1}(\eta,\zeta,\chi,\gamma,\phi) = \begin{pmatrix} 1 & 0 & 0 & 0 \\ 0 & e^{-i(\gamma+\zeta)}\cos\eta & -ie^{-i(\gamma-\chi)}\sin\eta & 0 \\ 0 & -ie^{-i(\gamma+\chi)}\sin\eta & e^{-i(\gamma-\zeta)}\cos\eta & 0 \\ 0 & 0 & 0 & e^{-i(2\gamma+\phi)} \end{pmatrix}, \tag{59}$$

in the basis of $\{|00\rangle, |01\rangle, |10\rangle, |11\rangle\}$, where η, ζ, χ, γ, and ϕ denote the variational parameters. This form is chosen so that $V^{(2)}_{j,j+1}$ can represent any two-qubit gate preserving the total Z spin, which is a symmetry of $H_{\rm AFM}$ [6,10]. We note that the brickwork structure of the ansatz with depth d is the same as that of the standard Trotterization,

$$U^{(L)}_{{\rm trot},d} \equiv \left(e^{-iH^{(L)}_{\rm even}\tau/d}e^{-iH^{(L)}_{\rm odd}\tau/d}\right)^d, \tag{60}$$

where $H_{\rm odd}$ [$H_{\rm even}$] represents terms composed of interactions between $(2k-1)$th and $2k$th sites [$2k$th and $(2k+1)$th sites] in $H_{\rm AFM}$. The depth-d ansatz includes the Trotterization with the same depth. Expecting the approximate translation symmetry of the model, we employ a single parameter set $(\eta,\zeta,\chi,\gamma,\phi)$ within each layer. With this setup, the number of independent variational parameters becomes $10d$ for the depth-d ansatz.

We examine how $U^{(L)}$ is approximated by the shallow-depth circuit $V^{(L)}(\theta_{\rm opt})$ with the optimal parameter set obtained in the smaller size $\tilde{L}$ and compare its performance with that of Trotterization. We assess them for different depths determined on the basis of the number of two-qubit gates as Eqs. (22) and (60), in which we do not take any hardware-specific detail into account. For the optimization in LVQC, we apply the protocol for translationally invariant systems under PBC based on the approximate translation symmetry of the model. To be precise, based on Theorem 4, we minimize the local cost function $C^{(\tilde{L}/2)}_{\rm LHST}(U^{(\tilde{L})}, V^{(\tilde{L})}(\theta))$, which is expected to approximate the local-compilation cost function $C^{(\tilde{L})}_{\alpha=0}(\theta)$. Then, with the optimal parameters $\theta_{\rm opt}$, we compute the cost functions

$C_{\mathrm{LHST}}(U^{(L)}, V^{(L)}(\theta_{\mathrm{opt}}))$ and $C_{\mathrm{LHST}}(U^{(L)}, V^{(L)}(\theta_{\mathrm{opt}}))$ to evaluate how well the ansatz $V^{(L)}(\theta_{\mathrm{opt}})$ reproduces $U^{(L)}$. We deal with size $L = 40$, time $\tau = 0.5$, and an ansatz depth d up to 5.

First, we show the numerical results for the depth compression in the intermediate size $\tilde{L}$. The compilation size $\tilde{L} = 2\lceil l_0 + d_H + v\tau + d' + 1/2 \rceil$ should be at least as large as $d_H + v\tau + 2d$ under $d = L'/4 + d'$. The AFM Heisenberg Hamiltonian $H^{(L)}_{\mathrm{AFM}}$ has the range of interactions, $d_H = 1$, and now we are assuming that $d = 5$. Since $v\tau$ is expected to be not so large under $\tau = 0.5$, we choose $\tilde{L} = 20$. We compute the cost function $C^{(\tilde{L}/2)}_{\mathrm{LHST}}(U^{(\tilde{L})}, V^{(\tilde{L})})$ based on Eq. (8) with a $2\tilde{L}$-qubit MPS. The bond dimension b for the MPS is determined so that the entanglement entropy during the dynamics, given by $S(\tau) \lesssim$ constant $\times$ τ in this model, becomes smaller than $\log_2 b$. We choose the bond dimension $b = 30$ here, since we confirm that it can accurately reproduce the dynamics with the larger bond dimension up to 60 or the exact dynamics of smaller systems up to 12 sites. For implementing $U^{(\tilde{L})}$, we employ the Trotterization $U^{(\tilde{L})}_{\mathrm{trot},d}$ with a sufficiently large depth $d = 100$. We variationally minimize the cost function by the Broyden-Fletcher-Goldfarb-Shanno (BFGS) method implemented in SciPy [57] with the maximum iteration set to 128. The initial parameter set θ is chosen as θ^d_{trot}, so that the ansatz $V(\theta^d_{\mathrm{trot}})$ becomes equivalent to the Trotterization with the same depth, $U_{\mathrm{trot},d}$, except for the global phase.

Figure 6(a) shows the history of the cost function during the optimization in $\tilde{L} = 20$, represented by the yellow ($d = 3$), blue ($d = 4$), and red ($d = 5$) solid lines in the panel. For comparison, we also compute the cost functions for shallow-depth Trotterization $C^{(\tilde{L}/2)}_{\mathrm{LHST}}(U^{(\tilde{L})}, V^{(\tilde{L})}(\theta^d_{\mathrm{trot}}))$ with various values of d, as described by the dashed lines. For each depth $d = 3$, 4, and 5, the ansatz with the resulting optimal parameter set θ_{opt} overwhelms the same-depth Trotterization. For instance, the depth-5 ansatz $V^{(\tilde{L})}(\theta_{\mathrm{opt}})$ provides the cost value 7.80×10^{-5}, which is as large as that for the depth-40 Trotterization, 8.48×10^{-5}. In other words, we successfully compress the time-evolution operator from depth 40 to depth 5 under compilation size $\tilde{L} = 20$.

Next, we examine how the larger-scale time-evolution operator $U^{(L)}$ is approximated by our protocol. Hereafter, we concentrate on the depth-5 ansatz and employ the corresponding optimal parameter set as θ_{opt}. Considering the approximate translation invariance, the size-extended ansatz $V^{(L)}(\theta_{\mathrm{opt}})$ is constructed by copying the two-qubit gate of $V^{(\tilde{L})}(\theta_{\mathrm{opt}})$ in the spatial direction. We again approximate $U^{(L)}$ by the large-depth Trotterization $U^{(L)}_{\mathrm{trot},d=100}$ and compute the cost functions as described in Fig. 6(b). As stated in Theorem 4, the local cost functions C_{LHST} and $C^{(L/2)}_{\mathrm{LHST}}$ (the purple and brown solid lines) hardly increase when we employ θ_{opt} in $\tilde{L} = 20$ for the larger-scale ansatz with $L \geq 20$. Reflecting the fact that Theorem 4 yields the loose bound proportional to L, the global cost function C_{HST} (the red solid line) experiences a gradual increase in L but remains sufficiently small compared to 1. Any cost function for the ansatz with θ_{opt} is comparably smaller than that with $\theta^{d=5}_{\mathrm{trot}}$, the parameter set for reproducing the Trotterization with the same depth, $d = 5$ (see the blue, orange, and light-green solid lines).

We also assess the average gate fidelity. Based on Eqs. (12) and (13), we ensure that the ansatz extended to $L = 40$ qubits has $\bar{F}(U^{(L)}, V^{(L)}(\theta_{\mathrm{opt}})) \geq 0.9977$, while the same-depth Trotterization provides $\bar{F}(U^{(L)}, V^{(L)}(\theta^{d=5}_{\mathrm{trot}})) \geq 0.8580$. Therefore, our protocol succeeds in implementing the time-evolution operator for the larger-scale $20 \leq L \leq 40$ with the limited depth by exploiting the local compilation on the size $\tilde{L} = 20$.

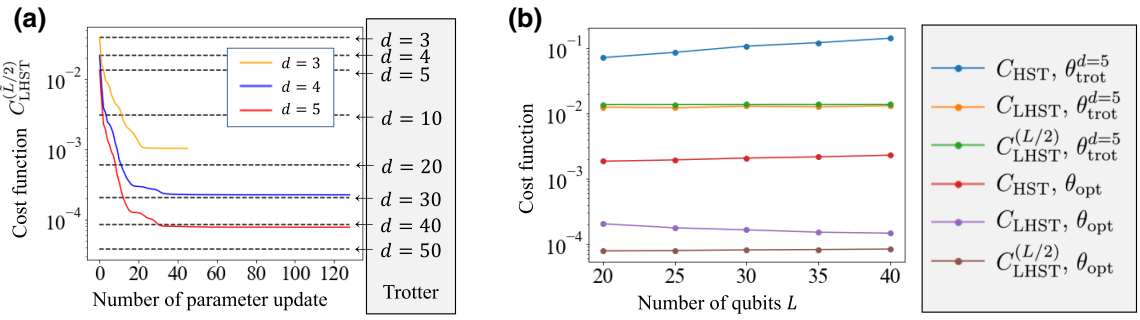

FIG. 6. (a) The history of the cost function $C^{(\tilde{L}/2)}_{\mathrm{LHST}}(U^{(\tilde{L})}, V^{(\tilde{L})}(\theta))$ in the intermediate size $\tilde{L} = 20$. The yellow, blue, and red solid lines, respectively, represent the results for the depth of the ansatz $d = 3, 4, 5$. The dashed lines represent the corresponding cost functions for the Trotterization with various depths d. (b) The cost functions $C(U^{(L)}, V^{(L)}(\theta))$ for increasing L. The ansatz compiled by LVQC, $V^{(L)}(\theta_{\mathrm{opt}})$, is obtained by the optimization using only $\tilde{L} = 20$ qubits. We evaluate the depth-5 LVQC result and the depth-5 Trotterization by $\theta^{d=5}_{\mathrm{trot}}$, by comparing the same kind of cost functions (e.g., the blue one should be compared with the red one). For any choice of the cost functions, LVQC achieves an approximately 100 times smaller value of the cost function than that of Trotterization.

Finally, we demonstrate how well the compressed time-evolution operator $V^{(L)}(\theta_{\rm opt})$ reproduces the dynamics of larger-scale systems under the exact time-evolution operator $U^{(L)}$. By applying $V^{(L)}(\theta_{\rm opt})$ or its inverse repeatedly, we can approximately simulate the stroboscopic dynamics at time $t \in \tau\mathbb{Z}$, which is larger than the original time scale τ, with a smaller-depth circuit. Furthermore, it should be noted that our protocol can capture larger-scale phenomena in the size L despite the compilation in $\tilde{L} < L$. To confirm this numerically, we simulate the stroboscopic dynamics, which involve a time scale and a size scale larger than $\tau = 0.5$ and $\tilde{L} = 20$, respectively.

As the simplest cases, we prepare the following two initial states:

$$|\psi^{(L)}_{\rm LE}(0)\rangle = X_{(L-\tilde{L})/2} X_{(L+\tilde{L})/2} |0\rangle^{\otimes L}, \tag{61}$$

$$|\psi^{(L)}_{\rm DW}(0)\rangle = \left(\prod_{j=(L-\tilde{L})/2}^{(L+\tilde{L})/2} X_j \right) |0\rangle^{\otimes L}, \tag{62}$$

for the size $L = 40$. They, respectively, represent ferromagnetic states having two local excitations (for $|\psi_{\rm LE}(0)\rangle$) and two domain walls (for $|\psi_{\rm DW}(0)\rangle$) with distance $\tilde{L} = 20$. Then, we evaluate the expectation value of $Z_{L/2}$ evolving under the Hamiltonian $H^{(L)}_{\rm AFM}$. Intuitively, it is expected that two distant local excitations or domain walls at the $(L-\tilde{L})/2$th and $(L+\tilde{L})/2$th sites, respectively, propagate in both left and right directions under the Hamiltonian $H^{(L)}_{\rm AFM}$ and the central site $j = L/2$ observes their collisions. Thus, the change in the expected value of $Z_{L/2}$ can be employed as a diagnosis for the larger-scale dynamics involving at least $\tilde{L}+1$ sites, which is larger than the compilation size.

Figure 7 shows the numerical results for the approximate stroboscopic dynamics obtained by the compilation. With the depth-5 ansatz $V^{(L)}(\theta_{\rm opt})$ obtained by the optimization in the size $\tilde{L} = 20$, we compute the state and its local observable, given by

$$|\psi^{(L)}(n\tau)\rangle = V^{(L)}(\theta_{\rm opt})^n |\psi^{(L)}(0)\rangle, \quad n \in \mathbb{N}, \tag{63}$$

$$Z_{L/2}(n\tau) = \langle \psi^{(L)}(n\tau) | Z_{L/2} | \psi^{(L)}(n\tau) \rangle. \tag{64}$$

We employ MPS with the bond dimension 60 for simulating the dynamics from the initial states $|\psi_{\rm LE}(0)\rangle$ or $|\psi_{\rm DW}(0)\rangle$, which are depicted as orange dots in Figs. 7(a) and 7(b), respectively. We also compute the dynamics under the large-depth Trotterization $U^{(L)}_{{\rm trot},d=100}$ as the accurate dynamics for the comparison (see the blue solid lines). In both cases, the compilation results reproduce the accurate dynamics well up to $t \le 10\tau = 5$, with the mean-square errors 5.27×10^{-6} and 1.29×10^{-6} [58]. We conclude that our prescription exploiting the intermediate-size $\tilde{L}$ and the fixed time τ provides an appropriate shallow-depth time-evolution operator that is useful for larger-scale

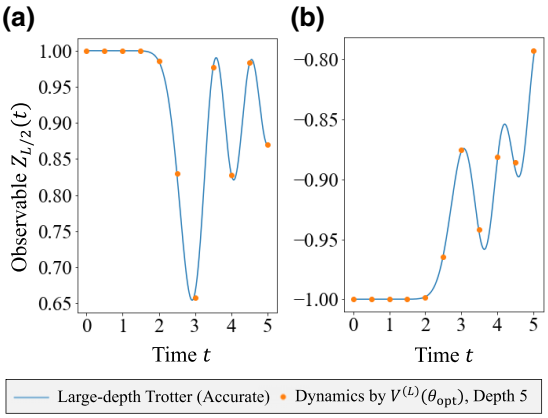

FIG. 7. The real-time dynamics of $Z_{L/2}$ (a) from the ferromagnetic initial state with two local excitations $|\psi^{(L)}_{\rm LE}(0)\rangle$ and (b) from the one with two domain walls $|\psi^{(L)}_{\rm DW}(0)\rangle$. The orange dots represent the stroboscopic dynamics at $t \in \tau\mathbb{Z}$ under $V^{(L)}(\theta_{\rm opt})$, implemented with the depth 50 up to $t = 5$. This well corresponds to the blue line, which shows accurate dynamics under the Trotterization with sufficiently large depth 100 per $\tau = 0.5$.

quantum systems in both space and time. We also remark that the optimal parameter obtained here is expected to be useful for even larger-scale quantum simulations beyond the size considered in this work, from the size dependence in Fig. 6(b). Our numerical results suggest the feasibility of using the classical local compilation to design large-scale quantum circuits, in addition to the possible quantum local compilation by NISQ devices.

VI. DISCUSSION AND CONCLUSIONS

In this paper, we develop LVQC, in which we conduct local optimization for intermediate-scale quantum systems designated by the Lieb-Robinson bound and obtain an approximate time-evolution operator of larger-scale quantum systems. Since the approximation error of the local cost function supporting our protocol relies only on the Lieb-Robinson bound, it has broad applicability to finite-ranged, short-ranged, and long-ranged interacting large-scale systems in generic dimensions. LVQC begins with the local compilation by intermediate-scale quantum devices or corresponding classical simulators and ends up with the quantum execution of the compiled larger-scale dynamics. Therefore, not only it unveils a classical approach to designing large-scale quantum circuits but it should also play a significant role in bridging the gap between NISQ device techniques and the practical use of larger quantum devices as the long-term goal.

We end this paper by providing some future directions. The first is to seek for the possibility of the local compilation in classical ways. While we refer to our protocol as "quantum" compilation, Theorems 4 and 5 are not

limited to the context of variational quantum algorithms, where we optimize a parametrized quantum circuit in a quantum-classical hybrid manner. Our numerical demonstration based on TEBD involving up to 40 qubits is indeed a good example for using a classical simulator for LVQC. Other sophisticated techniques [e.g., tensor-network-based methods for two-dimensional (2D) systems] will also be important for executing our protocol on classical computers. In future, we might also be able to use exact brute-force classical simulators for LVQC. This is because, for finite-ranged or short-ranged systems with $v\tau = O(L^0)$, LVQC ensures the classical efficient evaluation of the cost function in time $e^{O(\tilde{L})} = \mathrm{poly}(L)$ given that it is sufficient to take $\tilde{L} = O(\log L)$ in this case. Although current classical devices are still not capable of simulating quantum systems with size $\tilde{L}$, which typically becomes more than tens of qubits, in future LVQC may be available without resorting to approximate simulators. Note that this does not contradict the existing result, which states that the evaluation of the cost functions C_{LHST} and C_{HST} in polynomial accuracy with respect to the system size L for general unitaries is a DQC1-hard problem [37] (DQC1 refers to problems that are efficiently solvable by one clean qubit and other noisy qubits [59]), since we restrict ourselves to certain short-time local Hamiltonian dynamics and shallow depth ansatzes (for details, see Appendix C).

The second significant task for the future is to apply LVQC to various problems in condensed-matter physics and quantum chemistry, including higher-dimensional cases, short-ranged interacting cases, and long-ranged interacting cases. Several programmable quantum simulators, such as superconducting qubits [60] and Rydberg atoms [61], have recently achieved a few hundred qubits with high controllability and two dimensionality and they will be available for both the local compilation and the quantum execution of the compressed time evolution. For instance, it may be possible to observe long-time dynamics beyond the current coherence time on such compiled quantum simulators by the classical local compilation for tens of qubits. While the current knowledge of the LR bound and thereby LVQC can cover a variety of models in condensed-matter physics (e.g., the Hubbard model), it is also of great importance to explore the performance of LVQC for quantum chemistry problems such as molecules and crystals. Although we lack knowledge about the LR bound for the bare Coulomb interaction of approximately $1/r$, we can also try the protocol itself for such systems. Considering that the Coulomb interaction is often screened by electrons and nuclei and that several methods relying on the locality (e.g., the density-matrix renormalization group [62,63] and the divide-and-conquer method [64]) are successful, our LVQC will serve such structured quantum materials as a tool to accurately and efficiently extract their properties by the power of quantum computers.

ACKNOWLEDGMENTS

Kaoru Mizuta is supported by the "World-leading Innovative & Smart Education" (WISE) Program of the Ministry of Education, Culture, Sports, Science, and Technology (MEXT) and a Research Fellowship for Young Scientists from the Japan Society for the Promotion of Science (JSPS) (Grant No. JP20J12930). Kosuke Mitarai is supported by Japan Science and Technology Agency (JST) Precursory Research for Embryonic Science and Technology (PRESTO) Grant No. JPMJPR2019 and JSPS KAKENHI Grant No. 20K22330. Keisuke Fujii is supported by JST Exploratory Research for Advanced Technology (ERATO) Grant No. JPMJER1601 and JST Core Research for Evolutionary Science and Technology (CREST) Grant No. JPMJCR1673. This work is supported by MEXT Quantum Leap Flagship Program (MEXTQLEAP) Grants No. JPMXS0118067394 and No. JPMXS0120319794. We also acknowledge support from the JST COI-NEXT program Grant No. JPMJPF2014. Part of this work was performed for the Council for Science, Technology, and Innovation (CSTI), Cross-Ministerial Strategic Innovation Promotion Program (SIP), "Photonics and Quantum Technology for Society 5.0" (Funding agency: QST).

APPENDIX A: PROOF OF LEMMA 1

The quantity that we wish to evaluate is

$$\langle \Pi_j \rangle = \langle \Phi_+|_{AB} (U_A \otimes V_B^*)^\dagger \Pi_j (U_A \otimes V_B^*) |\Phi_+\rangle_{AB} . \quad \text{(A1)}$$

Noting that $(U_A \otimes V_B^*)|\Phi_+\rangle_{AB} = (U_A V_A^\dagger \otimes I_B)|\Phi_+\rangle_{AB}$ and Π_j can be decomposed as a sum of Pauli operator by Eq. (29), it is sufficient to evaluate

$$\langle \Phi_+|_{AB} (V_A U_A^\dagger \otimes I_B)(O_{A_j} \otimes O_{B_j})(U_A V_A^\dagger \otimes I_B) |\Phi_+\rangle_{AB} , \quad \text{(A2)}$$

for $O = X, Y, Z$ to obtain $\langle \Pi_j \rangle$. Therefore, if we have efficient means to evaluate

$$F(W_A, P_A, P_B) := \langle \Phi_+|_{AB} (W_A^\dagger \otimes I_B) P_A \otimes P_B (W_A \otimes I_B) |\Phi_+\rangle_{AB} \quad \text{(A3)}$$

for arbitrary L-qubit unitary W_A and Pauli operator P_A and P_B, we can obtain $\langle \Pi_j \rangle$. Here, we provide an efficient algorithm to estimate Eq. (A3).

First, we observe that the following equality holds:

$$F(W_A, P_A, P_B) = \frac{1}{2^L} \sum_{i,j=1}^{2^L} \langle i|_A W_A^\dagger P_A W_A |j\rangle_A \langle i|_B P_B |j\rangle_B \quad \text{(A4)}$$

$$= \frac{1}{2^L} \sum_{i,j=1}^{2^L} \mathrm{Re}\left[\langle i|_A W_A^\dagger P_A W_A |j\rangle_A \langle i|_B P_B |j\rangle_B \right], \quad \text{(A5)}$$

where we use the definition of the Bell state $|\Phi_+\rangle_{AB} = \sum_{i=1}^{2^L} |i\rangle_A |i\rangle_B / \sqrt{2^L}$ and that $F(W_A, P_A, P_B)$ is real. Now, a Monte Carlo approach can be employed to evaluate the sum of Eq. (A5).

The algorithm that we propose is as follows. First, sample x from the uniform distribution on $\{1, 2, \ldots, 2^L\}$. Let $\alpha_x |y_x\rangle = P_B |x\rangle$, where $|y_x\rangle$ and $\alpha_x \in \{\pm 1, \pm i\}$ is a computational basis and a coefficient determined by x and P_B. Then, we estimate $\langle y_x| W_A^\dagger P_A W_A |x\rangle$ on an L-qubit quantum device within an additive error ϵ. This can be achieved by utilizing the following equalities that hold for an arbitrary observable O:

$$2\mathrm{Re}[\langle y| O |x\rangle] = \langle +_{x,y}| O |+_{x,y}\rangle - \langle -_{x,y}| O |-_{x,y}\rangle, \quad \text{(A6)}$$

$$2\mathrm{Im}[\langle y| O |x\rangle] = \langle +i_{x,y}| O |+i_{x,y}\rangle - \langle -i_{x,y}| O |-i_{x,y}\rangle, \quad \text{(A7)}$$

where $|\pm_{x,y}\rangle := (|x\rangle \pm |y\rangle)/\sqrt{2}$ and $|\pm i_{x,y}\rangle := (|x\rangle \pm i|y\rangle)/\sqrt{2}$. More precisely, for a given pair (x, y_x), we first evaluate expectation values $\langle \pm_{x,y_x}| W_A^\dagger P_A W_A |\pm_{x,y_x}\rangle$ or $\langle \pm i_{x,y_x}| W_A^\dagger P_A W_A |\pm i_{x,y_x}\rangle$ using N_1 samples each and then combine them according to the above formula. Let an estimator of $\langle y_x| W_A^\dagger P_A W_A |x\rangle$ obtained by this procedure be $\hat{P}_{A,x}$. Importantly, $\mathrm{Var}[\hat{P}_{A,x}] = \mathcal{O}(1/N_1)$. Finally, we construct an estimator of $F(W_A, P_A, P_B)$ as

$$\hat{F}(W_A, P_A, P_B) := \mathrm{Re}\left[\alpha_x \hat{P}_{A,x}\right]. \quad \text{(A8)}$$

From this form of the estimator, it is sufficient to evaluate only $\mathrm{Re}[\langle y| O |x\rangle]$ ($\mathrm{Im}[\langle y| O |x\rangle]$) by Eqs. (A6) and (A7) when α_x is real (imaginary). Note that $\hat{F}(W_A, P_A, P_B)$ is defined by two random variables, x and $\hat{P}_{A,x}$.

To see that $\hat{F}(W_A, P_A, P_B)$ is indeed an efficient unbiased estimator, we analyze its expectation value and variance. Let us assume that, for a fixed x, the random variable $\mathrm{Re}[\alpha_x \hat{P}_{A,x}]$ follows a probability distribution $p_x(a)$. The probability that $\hat{F}(W_A, P_A, P_B)$ takes a specific value f is given by $\sum_x p_x(f)/2^L$. Then, we can calculate $\mathbb{E}[\hat{F}(W_A, P_A, P_B)]$ and $\mathbb{E}[\hat{F}(W_A, P_A, P_B)^2]$ as follows:

$$\begin{aligned}
&\mathbb{E}[\hat{F}(W_A, P_A, P_B)] \\
&= \sum_x \sum_f f \frac{p_x(f)}{2^L} \\
&= \frac{1}{2^L} \sum_x \mathbb{E}_{a\sim p_x(a)}[a] \\
&= \frac{1}{2^L} \sum_x \mathrm{Re}\left[\langle y_x|_A W_A^\dagger P_A W_A |x\rangle_A \langle y_x|_B P_B |x\rangle_B \right] \\
&= \frac{1}{2^L} \sum_{x,y} \mathrm{Re}\left[\langle y|_A W_A^\dagger P_A W_A |x\rangle_A \langle y|_B P_B |x\rangle_B \right] \\
&= F(W_A, P_A, P_B), \quad \text{(A9)}
\end{aligned}$$

$$\begin{aligned}
&\mathbb{E}[\hat{F}(W_A, P_A, P_B)^2] \\
&= \sum_x \sum_f f^2 \frac{p_x(f)}{2^L} \\
&= \frac{1}{2^L} \sum_x \left[\mathrm{Var}_{a\sim p_x}[a] + \sum_x \mathbb{E}_{a\sim p_x}[a]^2 \right] \\
&\le \max_x \mathrm{Var}_{a\sim p_x}[a^2] \quad \text{(A10)}
\end{aligned}$$

$$+ \frac{1}{2^L} \sum_x \mathrm{Re}\left[\langle y_x|_A W_A^\dagger P_A W_A |x\rangle_A \langle y_x|_B P_B |x\rangle_B \right]^2. \quad \text{(A11)}$$

Equation (A9) shows that $\hat{F}(W_A, P_A, P_B)$ is an unbiased estimator of $F(W_A, P_A, P_B)$, the desired quantity. Combining the above with

$$\mathrm{Var}_{a\sim p_x(a)}[a^2] = \mathbb{E}[a^2] - \langle y_x| W_A^\dagger P_A W_A |x\rangle^2 = \mathcal{O}(1/N_1) \quad \text{(A12)}$$

for all x, we obtain

$$\mathrm{Var}[\hat{F}(W_A, P_A, P_B)] \le \mathcal{O}(1/N_1) + \mathcal{V}, \quad \text{(A13)}$$

where

$$\begin{aligned}
\mathcal{V} := &\sum_x \mathrm{Re}\left[\langle y_x|_A W_A^\dagger P_A W_A |x\rangle_A^2 \langle y_x|_B P_B |x\rangle_B \right]^2 \\
&- \left(\sum_x \mathrm{Re}\left[\langle y_x|_A W_A^\dagger P_A W_A |x\rangle_A \langle y_x|_B P_B |x\rangle_B \right] \right)^2 \quad \text{(A14)}
\end{aligned}$$

is the variance of this protocol when we can exactly estimate $\mathrm{Re}[\langle y_x|_A W_A^\dagger P_A W_A |x\rangle_A \langle y_x|_B P_B |x\rangle_B]$.

Since $\mathrm{Re}[\langle y_x|_A W_A^\dagger P_A W_A |x\rangle_A \langle y_x|_B P_B |x\rangle_B] = \mathcal{O}(1)$, $\mathcal{V}$ is also $\mathcal{O}(1)$. This implies that a sample mean of N_2 independent samples of $\hat{F}(W_A, P_A, P_B)$, which requires $N = N_1 N_2$ runs of quantum devices for its construction, has variance $\mathcal{O}(1/(N_1 N_2)) + \mathcal{O}(1/N_2)$. Therefore, it is sufficient to take $N_1 = \mathcal{O}(1)$, $N_2 = \mathcal{O}(1/\epsilon^2)$ and thus $N = \mathcal{O}(1/\epsilon^2)$ to obtain an estimate of $F(W_A, P_A, P_B)$ within an additive error ϵ with high probability.

The same strategy can be adopted to evaluate $C_{\mathrm{HST}}(U,V)$. In this case, the task is to estimate the expectation value of $\Pi_1\Pi_2\cdots\Pi_L$ with respect to $(U_A\otimes V_B^*)\,|\Phi_+\rangle_{AB}$. We use the fact that $\Pi_1\Pi_2\cdots\Pi_L$ can also be expanded as a sum of Pauli operators:

$$\Pi_1\Pi_2\cdots\Pi_L=\frac{1}{4^L}\sum_{P\in\{I,X,Y,Z\}^{\otimes L}}c_P P\otimes P, \tag{A15}$$

where $c_P=1$ when P has an even number of Y and $c_P=-1$ otherwise. This decomposition has an exponential number of Pauli operators and a naive approach where we estimate expectation values of every Pauli operator takes exponential time to L. However, we can take a Monte Carlo approach to evaluating this sum by interpreting the coefficient $1/4^L$ as a probability.

The algorithm for evaluating $C_{\mathrm{HST}}(U,V)$ is as follows. First, we pick up a Pauli operator $P\in\{I,X,Y,Z\}^{\otimes L}$ randomly. Then, we estimate the expectation value of $P\otimes P$ using the algorithm in the proof of Lemma 1. Repeating the above procedure $N_3=\mathcal{O}(1/\epsilon^2)$ times while setting $N_1,N_2=\mathcal{O}(1)$, we obtain $C_{\mathrm{HST}}(U,V)$ within an additive error ϵ with high probability, using $N=N_1N_2N_3=\mathcal{O}(1/\epsilon^2)$ samples in total.

APPENDIX B: EXTENSION TO OTHER CASES

In the main text, we mainly focus on 1D systems with finite-ranged interactions. Here, we discuss the extensions of our results to other cases in terms of the range of interactions and the dimension of systems.

From the derivation of Theorems 4 and 5 in the main text, the range of interactions and the dimension affect our results only via $\varepsilon_{\mathrm{LR}}$ in Eq. (20), which is derived from the LR bound. To be precise, we should change the choice of the intermediate size $L'=2(l_0+d_H+v\tau)$ or $\tilde{L}\geq L'+2d'+1$, which designates the restriction of the Hamiltonian and the ansatz, so that the bound $\varepsilon_{\mathrm{LR}}$ can be ignored. Thus, after deriving $\varepsilon_{\mathrm{LR}}$ caused by the Hamiltonian restriction in Appendix B 1, we devote Secs. B 2–B 4 to discussing an appropriate choice of the size for finite-ranged, short-ranged, and long-ranged cases in generic dimensions.

1. Hamiltonian restriction by Lieb-Robinson bound

We first discuss the error bound $\varepsilon_{\mathrm{LR}}$ in Eq. (20), caused by the restriction of Hamiltonian to local terms around a site j. Let us assume that a Hamiltonian H has the LR bound designated by

$$\|[e^{iH\tau}O_Xe^{-iH\tau},O_Y]\|\leq\|O_X\|\cdot\|O_Y\|\cdot\mathcal{C}(\mathrm{dist}(X,Y),\tau), \tag{B1}$$

for the local observables O_X and O_Y, the supports of which are, respectively, the subsets of the lattice, X and Y ($\subseteq\Lambda$). The distance between domains is defined by

$$\mathrm{dist}(X,Y)=\inf\{\mathrm{dist}(j,j')\,|\,j\in X,j'\in Y\}. \tag{B2}$$

We also define the distance between a site j and a domain Y by $\mathrm{dist}(j,Y)=\mathrm{dist}(X=\{j\},Y)$.

Assuming the existence of the LR bound, we consider the dynamics of the local observables. We define the restriction of the Hamiltonian $H^{(L)}=\sum_X h_X$ for generic D-dimensional systems by

$$H^{(L'j)}=\sum_{X;X\subseteq\Lambda_{L'j}}h_X, \tag{B3}$$

$$\Lambda_{L'j}=\{j'\in\Lambda\,|\,\mathrm{dist}(j,j')\leq L'/2\}, \tag{B4}$$

where L and L' ($\leq L$), respectively, represent the linear scales of the lattices Λ and $\Lambda_{L'j}$. It is expected that the dynamics of the local observables, $e^{iH^{(L)}\tau}O_je^{-iH^{(L)}\tau}$, are well described by the restricted Hamiltonian $H^{(L'j)}$ for sufficiently large L', and in fact, this has been proved in Refs. [44–46] for the finite-ranged and short-ranged cases. In order to cover long-ranged cases and make our paper self-contained, we summarize and rederive the result in a slightly different way below. After that, we derive a proper choice of the compilation size $\tilde{L}$ for finite-ranged, short-ranged, and long-ranged cases in generic dimensions.

Lemma 6. We assume the existence of the LR bound in the form of Eq. (B1) on the Hamiltonian $H^{(L)}$, and define the size of a domain $X\subseteq\Lambda$ by

$$r(X)=\max\{\mathrm{dist}(j,j')\,|\,j,j'\in X\}. \tag{B5}$$

When the function $\mathcal{C}(r,t)$ is monotonically decreasing in the distance r and monotonically increasing in the time τ, the inequality

$$\|e^{iH^{(L)}\tau}O_je^{-iH^{(L)}\tau}-e^{iH^{(L'j)}\tau}O_je^{-iH^{(L'j)}\tau}\|\leq\varepsilon_{\mathrm{LR}}, \tag{B6}$$

$$\varepsilon_{\mathrm{LR}}=C_1\int_{L'/2-r_H}^{\infty}r^{D-1}\mathcal{C}(r,\tau)dr+\varepsilon(r_H), \tag{B7}$$

$$\varepsilon(r_H)=C_2\sum_{i\in\Lambda_{L'j}}\sum_{X;X\ni i,r(X)>r_H}\|h_X\| \tag{B8}$$

is satisfied, where the length scale r_H is an arbitrary value satisfying $0\leq r_H\leq L'/2$, and the constants C_1 and C_2 are independent of L and L'.

Proof. The proof is mainly based on Ref. [50] but we make a slight change so that it can cover short-ranged and long-ranged interactions. First, we define a function $f(t)$ by

$$f(t) = O_j - U_t^{(L',j)} U_t^{(L)\dagger} O_j U_t^{(L)} U_t^{(L',j)\dagger}, \tag{B9}$$

$$U_t^{(L)} = e^{-iH^{(L)}t}, \quad U_t^{(L',j)} = e^{-iH^{(L',j)}t}. \tag{B10}$$

$\|f(\tau)\|$ equals the left-hand side of Eq. (B6). Then, the differentiation of $f(t)$ in t immediately results in

$$f'(t) = iU_t^{(L',j)} \left[U_t^{(L)\dagger} O_j U_t^{(L)}, H^{(L)} - H^{(L',j)} \right] U_t^{(L',j)\dagger}. \tag{B11}$$

Considering that $f(0) = 0$, the operator norm $\|f(\tau)\|$ is bounded from above as follows:

$$\begin{aligned} \|f(\tau)\| &= \left\| \int_0^\tau f'(t)dt \right\| \le \int_0^\tau \left\| f'(t) \right\| dt \\ &= \int_0^\tau \left\| \left[U_t^{(L)\dagger} O_j U_t^{(L)}, H^{(L)} - H^{(L',j)} \right] \right\| dt. \end{aligned} \tag{B12}$$

From the definition of $H^{(L',j)}$, given by Eq. (B3), we obtain

$$H^{(L)} - H^{(L',j)} = \sum_{X; X \not\subseteq \Lambda_{L',j}} h_X. \tag{B13}$$

Introducing an arbitrary length scale r_H, satisfying $0 \le r_H \le L'/2$, the summation over X, which is not a subset of $\Lambda_{L',j}$, can be divided in the following way:

$$\sum_{X; X \not\subseteq \Lambda_{L',j}} = \sum_{X \in \mathcal{X}_A} + \sum_{X \in \mathcal{X}_B(r_H)} + \sum_{X \in \mathcal{X}_C(r_H)}, \tag{B14}$$

where each of $\mathcal{X}_A$, $\mathcal{X}_B(r_H)$, and $\mathcal{X}_C(r_H)$ is defined by

$$\mathcal{X}_A = \{X \,|\, X \subseteq \Lambda \backslash \Lambda_{L',j}\}, \tag{B15}$$

$$\mathcal{X}_B(r_H) = \{X \not\subseteq \Lambda_{L',j} \,|\, X \cap \Lambda_{L',j} \neq \phi,\, r(X) \le r_H\}, \tag{B16}$$

$$\mathcal{X}_C(r_H) = \{X \not\subseteq \Lambda_{L',j} \,|\, X \cap \Lambda_{L',j} \neq \phi,\, r(X) > r_H\}. \tag{B17}$$

Using the triangular inequality of the operator norm, Eq. (B12) is further bounded by

$$\|f(\tau)\| \le \varepsilon_{AB}(r_H) + \varepsilon_C(r_H), \tag{B18}$$

$$\varepsilon_{AB}(r_H) = \sum_{X \in \mathcal{X}_A \cup \mathcal{X}_B(r_H)} \int_0^\tau \left\| \left[U_t^{(L)\dagger} O_j U_t^{(L)}, h_X \right] \right\| dt, \tag{B19}$$

$$\varepsilon_C(r_H) = \sum_{X \in \mathcal{X}_C(r_H)} \int_0^\tau \left\| \left[U_t^{(L)\dagger} O_j U_t^{(L)}, h_X \right] \right\| dt. \tag{B20}$$

We now evaluate the upper bound of $\varepsilon_{AB}(r_H)$ and that of $\varepsilon_C(r_H)$, respectively.

For the first term $\varepsilon_{AB}(r_H)$, we use the fact that a domain X, which belongs to $\mathcal{X}_A \cup \mathcal{X}_B(r_H)$, satisfies $\mathrm{dist}(j,X) \ge L'/2 - r_H$ from their constructions in Eqs. (B15) and (B16). Using the LR bound given in Eq. (B1) for the integrand, $\varepsilon_{AB}(r_H)$ is bounded by

$$\begin{aligned} &\sum_{X \in \mathcal{X}_A \cup \mathcal{X}_B(r_H)} \int_0^\tau \|O_j\| \cdot \|h_X\| \cdot \mathcal{C}(\mathrm{dist}(j,X), t) dt, \\ &\le \sum_{j'; \mathrm{dist}(j,j') \ge L'/2 - r_H} \|O_j\| \sum_{X; X \ni j'} \tau \|h_X\| \cdot \mathcal{C}(\mathrm{dist}(j,j'), \tau), \\ &\le g\tau \|O_j\| \sum_{j'; \mathrm{dist}(j,j') \ge L'/2 - r_H} \mathcal{C}(\mathrm{dist}(j,j'), \tau). \end{aligned} \tag{B21}$$

In the first inequality, we employ the monotonicity of $\mathcal{C}(r,t)$, which validates the replacement by $\mathcal{C}(\mathrm{dist}(j,X),t) \le \mathcal{C}(\mathrm{dist}(j,j'),\tau)$ for $X \ni j'$ and $t \le \tau$. For the second inequality, we use Eq. (15). Concerning the summation over j' in the last line, the number of sites j' satisfying $\mathrm{dist}(j,j') \simeq r$ is proportional to the surface area $S_D r^{D-1}$ under the finite density ρ. Thus, the summation $\sum_{j'; \mathrm{dist}(j,j') \ge L'/2 - r_H}$ is expected to be approximated by $\int_{L'/2 - r_H}^\infty dr \rho S_D r^{D-1}$. In fact, following this intuition, when $\mathcal{C}(r,t)$ is monotonically decreasing in r and the number of sites per volume is finite, there exists a positive constant C_3 such that

$$[\text{Eq. (B21)}] \le g\tau \|O_j\| \cdot C_3 \int_{L'/2 - r_H}^\infty r^{D-1} \mathcal{C}(r,\tau) dr, \tag{B22}$$

for generic D-dimensional systems [50]. Here, the constant C_3 depends only on the dimension and the density of the lattice but not on L and L'. Defining the constant C_1 by $C_1 = g\tau \|O_j\| C_3$, $\varepsilon_{AB}(r_H)$ is bounded from above by the first term in the right-hand side of Eq. (B7).

For the second term $\varepsilon_C(r_H)$, we soon arrive at

$$\begin{aligned} \varepsilon_C(r_H) &\le \sum_{X \in \mathcal{X}_C(r_H)} 2\tau \|O_j\| \cdot \|h_X\|, \\ &\le 2\tau \|O_j\| \sum_{i \in \Lambda_{L',j}} \sum_{X; X \ni i, r(X) > r_H} \|h_X\|, \end{aligned} \tag{B23}$$

where we use the definition of $\mathcal{X}_C(r_H)$, given in Eq. (B17), to derive the second inequality. When we choose a constant C_2 by $2\tau\|O_j\|$, which is independent of L and L', $\varepsilon_C(r_H)$ is bounded by $\varepsilon(r_H)$ [see Eq. (B8)] from above.

Combining these upper bounds for $\varepsilon_{AB}(r_H)$ and that of $\varepsilon_C(r_H)$, we obtain the bound $\|f(\tau)\| \le \varepsilon_{\mathrm{LR}}$ by taking $\varepsilon_{\mathrm{LR}}$ from Eq. (B7), thereby completing the proof of Lemma 6. ■

Let us discuss in what conditions we can extend our results to other cases. The change in the dimension and the range of interactions only affects the proper choice of the partial system size L', which designates the linear scale of the Hamiltonian restriction. Once L' is determined, the remaining protocol is completely the same as that of the 1D finite-ranged cases; we compile the dynamics using a quantum system with size $\tilde{L} \geq L' + 2d' + 1$ [$d = L'/4 + d'$: the depth of the variational quantum circuit $V(\theta)$]. Therefore, it is sufficient to make $\varepsilon_{\mathrm{LR}}$ small enough with a proper-size $\tilde{L}$ based on Theorems 4 and 5. Depending on the kind of observables on which we are focusing, we have different conditions. When considering local observables under the approximate circuit $V^{(L)}(\theta_{\mathrm{opt}})$, we require $\varepsilon_{\mathrm{LR}} \ll 1$ to keep the local cost functions small according to Eq. (41) or Eq. (52). In this case, to extend our results, it is thus sufficient to choose a sufficiently large L' that makes $\varepsilon_{\mathrm{LR}} \ll 1$ while keeping $L'/L < 1$, so that the compilation size is smaller than L. On the other hand, when a near-unity average gate fidelity is required for global observables, we require that $|\Lambda|\varepsilon_{\mathrm{LR}} \sim L^D\varepsilon_{\mathrm{LR}} \ll 1$ based on Eqs. (48) and (54). As a result, the sufficient condition in that case is to achieve $L^D\varepsilon_{\mathrm{LR}} \ll 1$ with a sufficiently large L' while keeping $L'/L < 1$. In the following subsections, we derive how $\varepsilon_{\mathrm{LR}}$ scales with respect to L' in finite-ranged, short-ranged, and long-ranged interacting cases to confirm that our protocol can be applied to these setups.

2. Finite-ranged cases in generic dimensions

We consider finite-ranged cases in generic dimensions. As introduced in Eq. (17), here we assume

$$h_X = 0, \quad \text{if}\ ^{\exists} j, j' \in X \,\text{such that}\, \mathrm{dist}(j, j') > d_H, \tag{B24}$$

where d_H designates the range of interactions. Finite-ranged interacting systems have the LR bound $\mathcal{C}(r,t) = C\exp -(r - vt)/\xi$ under a fixed time t, with some constants C, v, and ξ, as introduced in Eq. (18) [41].

Let us evaluate the bound $\varepsilon_{\mathrm{LR}}$. We set $L' = 2(l_0 + d_H + v\tau)$ with a tunable scale l_0 and choose the parameter r_H in Eq. (B7) as $r_H = d_H$ ($\leq L'/2$). From the assumption of the range of interactions, $\varepsilon(r_H)$, defined by Eq. (B8), vanishes. This results in the bound

$$\varepsilon_{\mathrm{LR}} = C_1 \int_{l_0 + v\tau}^{\infty} r^{D-1} e^{-(r - v\tau)/\xi} dr, \tag{B25}$$

reproducing Eq. (21) in the main text. With some elementary integration using the gamma functions, we arrive at

$$\varepsilon_{\mathrm{LR}} = C_1 e^{-l_0/\xi} \sum_{k=0}^{D-1} \frac{(D-1)!}{(D-1-k)!} (l_0 + v\tau)^{D-1-k} \xi^k. \tag{B26}$$

Since the term in the summation is a polynomial of degree $D-1$ in $l_0 + v\tau$, there exists a positive constant C_4 satisfying

$$\begin{aligned} \varepsilon_{\mathrm{LR}} &\leq C_4 (l_0 + v\tau)^{D-1} e^{-l_0/\xi} \\ &= C_4 \exp\left\{-l_0/\xi + (D-1)\log(l_0 + v\tau)\right\}. \end{aligned} \tag{B27}$$

Since $\varepsilon_{\mathrm{LR}}$ exponentially decays in l_0 with polynomial corrections, both $\varepsilon_{\mathrm{LR}}$ and $L^D\varepsilon_{\mathrm{LR}}$ can be arbitrarily small with sufficiently large L' such that $L'/L < 1$. Thus, we can apply the LVQC protocol to finite-ranged cases, including high-dimensional systems.

Next, let us discuss how to choose the appropriate compilation size $\tilde{L}$. When focusing on local observables, we demand $\varepsilon_{\mathrm{LR}} \ll 1$, which results in the following choice:

(1) Choose l_0 so that

$$\exp\left\{-l_0/\xi + (D-1)\log(l_0 + v\tau)\right\} \tag{B28}$$

can be ignored compared to 1.

(2) Choose the compilation size by means of $\tilde{L} = 2\lceil l_0 + d_H + v\tau + d' + 1/2 \rceil$.

To make Eq. (B28) small enough, l_0 should be at least as large as ξ, which is the localization length of the LR bound. Thus, our protocol typically requires the linear scale $\tilde{L} \gtrsim 2(\xi + d_H + v\tau + d')$ for evaluating the cost functions. High-dimensional cases with $D \geq 2$ have logarithmic corrections in its exponent. Although a larger linear scale is required compared to 1D cases, we can still expect considerable decrease in the size.

On the other hand, when considering global observables, we demand $L^D\varepsilon_{\mathrm{LR}} \ll 1$. This brings an additional exponent $D\log L$ to Eq. (B28). As a result, the typical size for compilation becomes $\tilde{L} \gtrsim 2(\xi + d_H + v\tau + d' + D\xi\log L)$ to ensure high average gate fidelity for larger quantum systems.

3. Short-ranged cases in generic dimensions

Let us discuss short-ranged interacting systems in generic dimensions. In these cases, the range of interactions is infinite but their strength is suppressed exponentially in the distance as

$$\sum_{X; X \ni j, j'} \|h_X\| \leq h \exp\left(-\mathrm{dist}(j, j')/\zeta\right), \quad {}^{\forall} j, j' \in \Lambda, \tag{B29}$$

with some positive constants h and ζ, for the Hamiltonian $H^{(L)} = \sum_X h_X$. The LR bound is the same as that of the finite-ranged cases, $\mathcal{C}(r,t) = C\exp -(r - vt)/\xi$ [44–46].

Now, we evaluate the bound $\varepsilon_{\mathrm{LR}}$ for short-ranged cases. We choose the size L' by $L' = 2(l_0 + r_H + v\tau)$ with two tunable parameters, l_0 and r_H. The first term of $\varepsilon_{\mathrm{LR}}$ in Eq. (B7) is the same as that of the finite-ranged cases,

resulting in the bound in Eq. (B27). The second term $\varepsilon(r_H)$ is then bounded by

$$\varepsilon(r_H) \le C_2 \sum_{i\in\Lambda_{L',j}} \sum_{i'\in\Lambda;\mathrm{dist}(i,i')>r_H} \sum_{X;X\ni i,i'} \|h_X\| \le C_2 h \sum_{i\in\Lambda_{L',j}} \sum_{i'\in\Lambda;\mathrm{dist}(i,i')>r_H} \exp\left(-\mathrm{dist}(i,i')/\zeta\right). \tag{B30}$$

We can again replace the summation over i and i' by integration over D-dimensional real space, like the derivation of Eq. (B22) from Eq. (B21). With the use of a proper positive constant C_5, independent of L and L', we arrive at the following bound:

$$\varepsilon(r_H) \le C_5 (L')^D (r_H)^{D-1} e^{-r_H/\zeta}. \tag{B31}$$

Finally, using the relation $L' = 2(l_0 + r_H + v\tau)$, $\varepsilon_{\mathrm{LR}}$ satisfies the following inequality:

$$\varepsilon_{\mathrm{LR}} \le C_4 (l_0 + v\tau)^{D-1} e^{-l_0/\xi} + C_6 (l_0 + r_H + v\tau)^D r_H^{D-1} e^{-r_H/\zeta}, \tag{B32}$$

where C_4 and C_6 are some positive constants independent of L and L'.

Similar to finite-ranged cases, both $\varepsilon_{\mathrm{LR}}$ and $L^D\varepsilon_{\mathrm{LR}}$ can be arbitrarily small with properly increasing l_0 and r_H under $L'/L < 1$. When we focus on local observables for larger-scale dynamics demanding $\varepsilon_{\mathrm{LR}} \ll 1$, we should choose the compilation size $\tilde{L}$ in the following way:

(1) Choose l_0 so that

$$\exp\{-l_0/\xi + (D-1)\log(l_0 + v\tau)\} \tag{B33}$$

can be ignored compared to 1.

(2) Choose r_H so that

$$\exp\left\{-\frac{r_H}{\zeta} + D\log(l_0 + r_H + v\tau) + (D-1)\log r_H\right\} \tag{B34}$$

can be ignored compared to 1, under the above choice of l_0.

(3) Choose the compilation size by means of $\tilde{L} = 2\lceil l_0 + r_H + v\tau + d' + 1/2\rceil$.

In contrast to finite-ranged cases, the error $\varepsilon_{\mathrm{LR}}$ always has logarithmic corrections in its exponent and has two independent tunable parameters for the scale $\tilde{L}$. To make both Eqs. (B33) and (B34) sufficiently small, the compilation size $\tilde{L}$ should be at least as large as $2(\xi + \zeta + v\tau + d')$, ζ being the typical range of interactions, which gives the typical size scale of short-ranged cases. When the high average gate fidelity is required, we replace the protocol by adding $D\log L$ to the exponents of Eqs. (B33) and (B34), to achieve $L^D\varepsilon_{\mathrm{LR}} \ll 1$. Then, the typical compilation size scale becomes $\tilde{L} \gtrsim 2\{\xi + \zeta + v\tau + d' + D(\xi + \zeta)\log L\}$.

4. Long-ranged cases in generic dimensions

The last case that we consider is a long-ranged Hamiltonian in generic dimensions. Here, we assume power-law interactions, satisfying

$$\sum_{X:X\ni j, r(X)\ge R} \|h_X\| \le \frac{h}{R^\alpha}, \quad {}^\forall j \in \Lambda, \tag{B35}$$

for any sufficiently large distance $R > 0$, where h and α denote some positive constants. One of the simplest cases is the long-ranged transverse Ising model defined by

$$H = \sum_{j,j'\in\Lambda, j\ne j'} \frac{Z_j Z_{j'}}{\mathrm{dist}(j,j')^{D+\alpha}} + \sum_{j\in\Lambda} X_j, \tag{B36}$$

on a D-dimensional lattice Λ. While a series of recent studies have succeeded in extending the LR bound to long-ranged cases in different ways [47–52], we hereby focus on one of their results, derived in Ref. [50]. When the power α is larger than the dimension D, there exist positive constants v, C_7, and C_8, such that

$$\mathcal{C}(r,\tau) \le C_7 \exp\left(v\tau - r^{1-\sigma}\right) + C_8 \frac{f_\sigma(v\tau)}{r^{\sigma\alpha}}, \tag{B37}$$

for any σ satisfying $(D+1)/(\alpha+1) < \sigma < 1$. Here, $f_\sigma(x)$ is a monotonically increasing function in x independent of L and can be regarded as a positive constant for fixed τ and σ.

We compute the upper bound of $\varepsilon_{\mathrm{LR}}$ based on Eq. (B7). The intermediate size L' is again given by $L' = 2(l_0 + r_H + v\tau)$ with two tunable parameters, l_0 and r_H. Substituting the above LR bound into Eq. (B7), the first term of Eq. (B7) is bounded by

$$\int_{l_0+v\tau}^\infty r^{D-1}\mathcal{C}(r,\tau)dr \le C_7 e^{v\tau} \int_{l_0+v\tau}^\infty r^{D-1} e^{-r^{1-\sigma}} dr + C_8 f_\sigma(v\tau) \int_{l_0+v\tau}^\infty r^{D-1-\sigma\alpha} dr. \tag{B38}$$

The first integral on the right-hand side is computed by the substitution of $s = r^{1-\sigma} - (l_0 + v\tau)^{1-\sigma}$, which results in

$$\begin{aligned} & C_7 e^{v\tau} \int_{l_0+v\tau}^{\infty} r^{D-1} e^{-r^{1-\sigma}} dr \\ &= \frac{C_7 e^{v\tau-(l_0+v\tau)^{1-\sigma}}}{1-\sigma} \\ &\quad \times \int_0^{\infty} \{s + (l_0+v\tau)^{1-\sigma}\}^{(D/(1-\sigma))-1} e^{-s} ds \\ &\le \frac{C_7 e^{v\tau-(l_0+v\tau)^{1-\sigma}}}{1-\sigma} \int_0^{\infty} \{s + (l_0+v\tau)^{1-\sigma}\}^{n_{D\sigma}-1} e^{-s} ds, \end{aligned} \tag{B39}$$

with $n_{D\sigma} = \lceil D/(1-\sigma) \rceil \in \mathbb{N}$. As we derive Eq. (B27) from Eq. (B25) using the gamma functions, there exists a positive constant C_9, which is dependent only on D and σ, such that

$$\begin{aligned} C_1 \times [\text{Eq. (B39)}] &\le C_9 e^{v\tau-(l_0+v\tau)^{1-\sigma}} (l_0+v\tau)^{n_{D\sigma}(1-\sigma)} \\ &\le C_9 e^{v\tau-(l_0+v\tau)^{1-\sigma}} (l_0+v\tau)^{D+1-\sigma} \end{aligned} \tag{B40}$$

is satisfied. On the other hand, considering $D - 1 - \sigma\alpha < -1$ from $(D+1)/(\alpha+1) < \sigma < 1$, the second integral on the right-hand side of Eq. (B38) is easily computed as

$$C_8 f_\sigma(v\tau) \int_{l_0+v\tau}^{\infty} r^{D-1-\sigma\alpha} dr = \frac{C_8 f_\sigma(v\tau)}{\sigma\alpha - D} (l_0+v\tau)^{D-\sigma\alpha}. \tag{B41}$$

We define a positive constant C_{10} by $C_{10} = C_8 f_\sigma(v\tau)/\{C_1(\sigma\alpha - D)\}$ and then Eqs. (B40) and (B41) imply that

$$\begin{aligned} & C_1 \int_{L'/2-r_H}^{\infty} r^{D-1} \mathcal{C}(r,\tau) dr \\ &\le C_9 e^{v\tau-(l_0+v\tau)^{1-\sigma}} (l_0+v\tau)^{D+1-\sigma} + C_{10}(l_0+v\tau)^{D-\sigma\alpha}. \end{aligned} \tag{B42}$$

We note that this bound is independent of L and vanishes with increasing $l_0 \to \infty$.

When the tunable parameter r_H is sufficiently large, the second term $\varepsilon(r_H)$, defined by Eq. (B8), immediately satisfies the following inequality:

$$\varepsilon(r_H) \le C_2 |\Lambda_{L',j}| \cdot \frac{h}{(r_H)^\alpha}, \tag{B43}$$

where we use the assumption of long-ranged interactions, given in Eq. (B35). Considering that the volume $|\Lambda_{L',j}|$ is proportional to $(L')^D$, there exists a positive constant C_{11} such that $\varepsilon(r_H) \le C_{11}(l_0 + r_H + v\tau)^D \cdot (r_H)^{-\alpha}$. From the assumption of $\alpha > D$, this bound vanishes under $r_H \to \infty$ when the other parameter l_0 is fixed.

Summarizing the results in Eqs. (B42) and (B43), we obtain the bound of $\varepsilon_{\mathrm{LR}}$ for long-ranged cases in generic dimensions as

$$\begin{aligned} \varepsilon_{\mathrm{LR}} &\le C_9 e^{v\tau-(l_0+v\tau)^{1-\sigma}+(D+1-\sigma)\log(l_0+v\tau)} \\ &\quad + C_{10}(l_0+v\tau)^{D-\sigma\alpha} + C_{11} \times \frac{(l_0+r_H+v\tau)^D}{(r_H)^\alpha}. \end{aligned} \tag{B44}$$

In contrast to the finite-ranged and short-ranged cases, the bound $\varepsilon_{\mathrm{LR}}$ shows polynomial decay in $\tilde{L}$, which leads to the absence of characteristic length. In addition, this also alters the applicability of the LVQC protocol depending on whether we focus on local or global observables for larger-scale systems.

When we are interested in local observables, $\varepsilon_{\mathrm{LR}} \ll 1$ is demanded. Since $\varepsilon_{\mathrm{LR}}$ is independent of L, we can make $\varepsilon_{\mathrm{LR}}$ arbitrarily small by increasing l_0 and r_H under the constraint $L'/L < 1$. We can apply the LVQC protocol as long as the LR bound exists (e.g., $\alpha > D$ is required when we employ the LR bound in Ref. [50]). The proper compilation size $\tilde{L}$ is organized into the following steps:

(1) Choose l_0 so that both of

$$e^{v\tau-(l_0+v\tau)^{1-\sigma}+(D+1-\sigma)\log(l_0+v\tau)} \tag{B45}$$

and $(l_0+v\tau)^{D-\sigma\alpha}$ become sufficiently small compared to 1.

(2) Choose r_H so that $(l_0+r_H+v\tau)^D/(r_H)^\alpha$ can be ignored compared to 1, under the above choice of l_0.

(3) Choose the compilation size by $\tilde{L} = 2\lceil l_0 + r_H + v\tau + d' + 1/2 \rceil$.

Here, we have options in the parameter σ satisfying $(D+1)/(\alpha+1) < \sigma < 1$. Since the constants C_9 and C_{10} are divergent for σ around its lower and upper bounds [see Eqs. (B39) and (B41)], a possible good choice may be $\sigma = \{(D+1)/(\alpha+1) + 1\}/2$.

When we are interested in global observables, we demand $L^D \varepsilon_{\mathrm{LR}} \ll 1$. The protocol to choose L' is largely the same as the above one, where each term in $\varepsilon_{\mathrm{LR}}$ is replaced by the corresponding term in $L^D \varepsilon_{\mathrm{LR}}$. However, due to the polynomial decay of $\varepsilon_{\mathrm{LR}}$ in l_0 and r_H, we should impose additional conditions on the exponents α and D. Let us discuss the asymptotic behavior of the compilation size by defining the scaling $l_0 \sim L^\beta$ and $r_H \sim L^\delta$ with $\beta, \delta < 1$. Multiplying the right-hand side of Eq. (B44) by L^D, we have three terms that should decay. The first term decays subexponentially in l_0 but polynomially increases in L. It can thus be made arbitrarily small by choosing sufficiently large l_0. With regard to the second term, we demand

the convergence of $L^D(l_0+v\tau)^{D-\sigma\alpha} \sim L^{D+\beta(D-\sigma\alpha)}$ (here, we assume that $v\tau$ is constant). As a result, the inequalities $\sigma\alpha - D > 0$ and

$$\frac{D}{\sigma\alpha - D} < \beta < 1 \tag{B46}$$

should be satisfied. The relation $\beta < 1$ ensures reduction in the compilation size. The above inequality implies that $\alpha > 2D$ and $\sigma > 2D/\alpha$ must be satisfied for successful size reduction. Finally, the third term scales as $L^{D\max(\beta,\delta)-\alpha\delta+D}$. Taking the above constraints on β and σ, the sufficient condition for the vanishing third term is to satisfy

$$\frac{\sigma D}{\sigma\alpha - D} < \delta < 1. \tag{B47}$$

To summarize, when demanding high average gate fidelity, we can apply LVQC to long-ranged interacting systems with the exponent $\alpha > 2D$, which is stricter than what is required for the existence of the LR bound. Then, the compilation size $\tilde{L}$ is at least proportional to $L^{D/(\sigma\alpha-D)}$ with $2D/\alpha < \sigma < 1$.

Let us finally discuss concrete examples of systems where we can apply LVQC successfully. With the usage of the LR bound for the long-ranged cases derived in Ref. [50], the constraint for the local observables, $\alpha > D$, tells us about the availability of LVQC to various systems, such as 1D systems with dipole-type interactions ($\alpha = 2, D = 1$) and 1D or 2D systems with van der Waals interactions ($\alpha = 5$, $D = 1$ or $\alpha = 4$, $D = 2$). On the other hand, the constraint on global observables, $\alpha > 2D$, implies applicability to limited cases, such as 1D systems with van der Waals interactions ($\alpha = 5, D = 1$) within the above examples. In both cases, the application to long-ranged Hamiltonians of electrons from first principles (i.e., $\alpha = 1 - D$ by Coulomb potentials) seems to be difficult with the current knowledge of the LR bound. Anyway, we expect applicability of LVQC to broader systems with the usage of other formulations on the LR bound [47–49,51,52] or as its further development.

APPENDIX C: RELATION TO DQC1 HARDNESS OF COMPUTING COST FUNCTIONS

In this appendix, we discuss how the LVQC protocol is related to the computational complexity of QAQC. According to Ref. [37], the determination of the cost functions belongs to DQC1-hard problems. This indicates that efficient QAQC by classical computers is difficult. On the other hand, our LVQC enables efficient evaluation of the cost functions with a restricted size $\tilde{L}$ and, in some cases, we can efficiently complete the protocol by MPS, as in Sec. V. Here, we resolve this apparent contradiction.

We first introduce the complexity class, DQC1 (deterministic quantum computation with one clean qubit) [59]. Here, we concentrate on a 1D system (extension to higher-dimensional systems is straightforward). In the DQC1 model, we prepare an $(L+1)$-qubit initial state, composed of one clean qubit and with the other qubits lying in a maximally mixed state, as

$$\rho = |0\rangle\langle 0| \otimes \left(\frac{|0\rangle\langle 0| + |1\rangle\langle 1|}{2}\right)^{\otimes L}. \tag{C1}$$

Then, we apply a unitary gate U with the depth up to poly(L) and obtain the following probability by measuring the first clean qubit,

$$p_z = \mathrm{Tr}[(|z\rangle\langle z|)_1 U\rho U^\dagger], \quad z = 0, 1. \tag{C2}$$

We refer to the problem of determining the probability p_z with a multiplicative error $\varepsilon < 1$ as the DQC1 model. DQC1 models were originally introduced to evaluate the power of nuclear-magnetic-resonance quantum computers. Famous examples of DQC1-complete problems are the estimation of spectral density [59], the trace of unitary matrices [65], and the Jones polynomials [66]. Importantly, in Ref. [67] it is proved that, if the probability p_z can be sampled with poly(L)-time classical algorithms, the polynomial hierarchy will collapse to the second level. This implies that efficiently simulating the DQC1 models in classical ways is unlikely. Recently, in Ref. [37] it has been revealed that the determination of the global cost function C_{HST} or the local one C_{LHST} with an error $\varepsilon < 1/\mathrm{poly}(L)$ is DQC1 hard for poly(L) depth unitaries U and V; any DQC1 model can be reduced to the problem of determining the above cost functions. Based on this fact, quantum compilation with the cost functions C_{HST} or C_{LHST} is also expected to be difficult by classical computation.

LVQC seems to give contradictory results due to the size reduction. Let us consider 1D systems with finite-ranged interactions and assume that the compilation size $\tilde{L} = 2\lceil l_0 + d_H + v\tau + d' + 1/2\rceil$ satisfies $\tilde{L} \propto \log L$. We can classically compute the cost function $C^{(\tilde{L})}(\theta)$ with accuracy $1/\mathrm{poly}(L)$ by employing matrices the dimension of which is $e^{O(\tilde{L})} \sim \mathrm{poly}(L)$ based on Eqs. (8) and (49). It takes at most poly(L) time for its classical evaluation. Considering that $\varepsilon_{\mathrm{LR}}$ is suppressed as $\varepsilon_{\mathrm{LR}} < e^{-O(\tilde{L})} = 1/\mathrm{poly}(L)$, Propositions 2 and 3 (or the proof for Theorem 5) say that

$$|C_{\mathrm{LHST}}(U^{(L)}, V^{(L)}(\theta)) - C^{(\tilde{L})}(\theta)| < \frac{3}{4}\varepsilon_{\mathrm{LR}} = 1/\mathrm{poly}(L). \tag{C3}$$

Therefore, we can classically determine the local cost function $C_{\mathrm{LHST}}(U^{(L)}, V^{(L)}(\theta))$ with polynomial time in the system size L. Does this imply the collapse of the

polynomial hierarchy or a fault in the LVQC formalism? As the discussion below shows, the LVQC protocol leads to neither conclusion.

We resolve the discrepancy depending on the size of the causal cones generated by the LR bound, $v\tau$. The first case is where the time τ is constant. Then, the time-evolution operator $U^{(L)} = e^{-iH^{(L)}\tau}$ is not universal under the locality. The LR bound allows us to regard it as a $O(L^0)$-depth circuit in terms of the local observable C_{LHST}. Therefore, while the local cost function $C_{\mathrm{LHST}}(U^{(L)}, V^{(L)}(\theta))$ can actually be obtained by poly(L)-time classical computation, this case is not problematic. The second case is $v\tau \propto L^{\kappa}$, where we can expect the size reduction if we assume $0 < \kappa < 1$. In that case, the compilation size $\tilde{L} = 2\lceil l_0 + d_H + v\tau + d'/2 \rceil$ is proportional to L^{κ} and cannot scale as $\log L$. Thus, the above discussion predicting the poly(L)-time classical evaluation is precluded, which results in the consistency of LVQC with the DQC1 hardness of determining the cost function C_{LHST}. Similarly, LVQC appears to allow classically efficient evaluation of the global cost function C_{HST} but there exists no conflict with its DQC1 hardness.

We emphasize some points throughout this discussion. First, in some cases, local compilation by classical computers remains possible. For finite-ranged or short-ranged interacting systems under $v\tau = O(L^0)$, LVQC can be completed with poly(L)-time classical computation. While we employ an approximate classical algorithm relying on the MPS in Sec. V, we expect that high-performance classical computers in the future will achieve the compilation for the size $\tilde{L} \sim \log L$ without resorting to any approximation. On the other hand, we also note that intermediate-scale quantum devices still play a significant role in the local compilation. While the compilation size $\tilde{L}$ scales as $\log L$ in the above cases under $L \to \infty$, the remaining constant term is not so small for current classical computers. For instance, as in the numerical simulation in Sec. V, a typical 1D spin chain with finite-ranged interactions requires $\tilde{L} = 20$, resulting in the compilation using 40-qubit quantum systems. It will be necessary to prepare hundreds or thousands of qubits for higher-dimensional systems involving finite-, short-, and long-ranged interactions. Since the DQC1 hardness denies poly$(\tilde{L})$-time classical simulation of the local compilation, NISQ devices will be essential to compile larger-scale time-evolution operators.

[1] J. Preskill, Quantum computing in the NISQ era and beyond, Quantum **2**, 79 (2018).

[2] S. Lloyd, Universal quantum simulators, Science **273**, 1073 (1996).

[3] A. Y. Kitaev, Quantum measurements and the Abelian Stabilizer problem, arXiv:quant-ph/9511026 [quant-ph] (1995).

[4] R. Cleve, A. Ekert, C. Macchiavello, and M. Mosca, Quantum algorithms revisited, Proc. R. Soc. London Ser. A **454**, 339 (1998).

[5] M. A. Nielsen and I. Chuang, *Quantum Computation and Quantum Information* (Cambridge University Press, Cambridge, UK, 2002).

[6] F. Arute, K. Arya, R. Babbush, D. Bacon, Joseph C. Bardin, R. Barends, A. Bengtsson, S. Boixo, M. Broughton, Bob B. Buckley, *et al.*, Observation of separated dynamics of charge and spin in the Fermi–Hubbard model, arXiv:2010.07965 [quant-ph] (2020).

[7] X. Mi, M. Ippoliti, C. Quintana, A. Greene, Z. Chen, J. Gross, F. Arute, K. Arya, J. Atalaya, R. Babbush, *et al.*, Time-crystalline eigenstate order on a quantum processor, Nature **601**, 531 (2021).

[8] J. Randall, C. E. Bradley, F. V. van der Gronden, A. Galicia, M. H. Abobeih, M. Markham, D. J. Twitchen, F. Machado, N. Y. Yao, and T. H. Taminiau, Many-body-localized discrete time crystal with a programmable spin-based quantum simulator, Science **374**, 1474 (2021).

[9] A. Smith, M. S. Kim, F. Pollmann, and J. Knolle, Simulating quantum many-body dynamics on a current digital quantum computer, npj Quantum Inf. **5**, 1 (2019).

[10] C. Neill, T. McCourt, X. Mi, Z. Jiang, M. Y. Niu, W. Mruczkiewicz, I. Aleiner, F. Arute, K. Arya, J. Atalaya, *et al.*, Accurately computing the electronic properties of a quantum ring, Nature **594**, 508 (2021).

[11] D. Zhu, S. Johri, N. H. Nguyen, C. H. Alderete, K. A. Landsman, N. M. Linke, C. Monroe, and A. Y. Matsuura, Probing many-body localization on a noisy quantum computer, Phys. Rev. A **103**, 032606 (2021).

[12] D. S. Abrams and S. Lloyd, Simulation of Many-Body Fermi Systems on a Universal Quantum Computer, Phys. Rev. Lett. **79**, 2586 (1997).

[13] A. T. Sornborger and E. D. Stewart, Higher-order methods for simulations on quantum computers, Phys. Rev. A **60**, 1956 (1999).

[14] E. Campbell, Random Compiler for Fast Hamiltonian Simulation, Phys. Rev. Lett. **123**, 070503 (2019).

[15] A. M. Childs, A. Ostrander, and Y. Su, Faster quantum simulation by randomization, Quantum **3**, 182 (2019).

[16] A. M. Childs, Y. Su, M. C. Tran, N. Wiebe, and S. Zhu, Theory of Trotter Error with Commutator Scaling, Phys. Rev. X **11**, 011020 (2021).

[17] Y. Ouyang, D. R. White, and E. T. Campbell, Compilation by stochastic Hamiltonian sparsification, Quantum **4**, 235 (2020).

[18] P. J. J. O'Malley, R. Babbush, I. D. Kivlichan, J. Romero, J. R. McClean, R. Barends, J. Kelly, P. Roushan, A. Tranter, N. Ding, *et al.*, Scalable Quantum Simulation of Molecular Energies, Phys. Rev. X **6**, 031007 (2016).

[19] B. P. Lanyon, C. Hempel, D. Nigg, M. Müller, R. Gerritsma, F. Zähringer, P. Schindler, J. T. Barreiro, M. Rambach, G. Kirchmair, M. Hennrich, P. Zoller, R. Blatt, and C. F. Roos, Universal digital quantum simulation with trapped ions, Science **334**, 57 (2011).

[20] G. H. Low and I. L. Chuang, Hamiltonian simulation by qubitization, Quantum **3**, 163 (2019).

[21] R. Babbush, C. Gidney, D. W. Berry, N. Wiebe, J. McClean, A. Paler, A. Fowler, and H. Neven, Encoding Electronic

Spectra in Quantum Circuits with Linear T Complexity, Phys. Rev. X **8**, 041015 (2018).
[22] E. Kökcü, D. Camps, L. Bassman, J. K. Freericks, W. A. de Jong, R. Van Beeumen, and A. F. Kemper, Algebraic compression of quantum circuits for Hamiltonian evolution, arXiv:2108.03282 [quant-ph] (2021).
[23] S. Gulania, B. Peng, Y. Alexeev, and N. Govind, Quantum time dynamics of 1D-Heisenberg models employing the Yang-Baxter equation for circuit compression, arXiv:2112.01690 [quant-ph] (2021).
[24] M. Cerezo, A. Arrasmith, R. Babbush, S. C. Benjamin, S. Endo, K. Fujii, J. R. McClean, K. Mitarai, X. Yuan, L. Cincio, *et al.*, Variational quantum algorithms, Nat. Rev. Phys. **3**, 625 (2021).
[25] Y. Li and S. C. Benjamin, Efficient Variational Quantum Simulator Incorporating Active Error Minimization, Phys. Rev. X **7**, 021050 (2017).
[26] X. Yuan, S. Endo, Q. Zhao, Y. Li, and S. C. Benjamin, Theory of variational quantum simulation, Quantum **3**, 191 (2019).
[27] K. Heya, K. M. Nakanishi, K. Mitarai, and K. Fujii, Subspace variational quantum simulator, arXiv:1904.08566 [quant-ph] (2019).
[28] S. Endo, J. Sun, Y. Li, S. C. Benjamin, and X. Yuan, Variational Quantum Simulation of General Processes, Phys. Rev. Lett. **125**, 010501 (2020).
[29] S. Endo, I. Kurata, and Y. O. Nakagawa, Calculation of the Green's function on near-term quantum computers, Phys. Rev. Res. **2**, 033281 (2020).
[30] M. Benedetti, M. Fiorentini, and M. Lubasch, Hardware-efficient variational quantum algorithms for time evolution, Phys. Rev. Res. **3**, 033083 (2021).
[31] S.-H. Lin, R. Dilip, A. G. Green, A. Smith, and F. Pollmann, Real- and Imaginary-Time Evolution with Compressed Quantum Circuits, PRX Quantum **2**, 010342 (2021).
[32] N. F. Berthusen, T. V. Trevisan, T. Iadecola, and P. P. Orth, Quantum dynamics simulations beyond the coherence time on NISQ hardware by variational Trotter compression, arXiv:2112.12654 [quant-ph] (2021).
[33] T. Jones and S. C. Benjamin, Robust quantum compilation and circuit optimisation via energy minimisation, Quantum **6**, 628 (2022).
[34] C. Cîrstoiu, Z. Holmes, J. Iosue, L. Cincio, P. J. Coles, and A. Sornborger, Variational fast forwarding for quantum simulation beyond the coherence time, npj Quantum Inf. **6**, 82 (2020).
[35] B. Commeau, M. Cerezo, Z. Holmes, L. Cincio, P. J. Coles, and A. Sornborger, Variational Hamiltonian diagonalization for dynamical quantum simulation, arXiv:2009.02559 [quant-ph] (2020).
[36] J. Gibbs, K. Gili, Z. Holmes, B. Commeau, A. Arrasmith, L. Cincio, P. J. Coles, and A. Sornborger, Long-time simulations with high fidelity on quantum hardware, arXiv:2102.04313 [quant-ph] (2021).
[37] S. Khatri, R. LaRose, A. Poremba, L. Cincio, A. T. Sornborger, and P. J. Coles, Quantum-assisted quantum compiling, Quantum **3**, 140 (2019).
[38] K. Sharma, S. Khatri, M. Cerezo, and P. J. Coles, Noise resilience of variational quantum compiling, New J. Phys. **22**, 043006 (2020).
[39] S. Bilek and K. Wold, Recursive variational quantum compiling, arXiv:2203.08514 [quant-ph] (2022).
[40] R. Mansuroglu, T. Eckstein, L. Nützel, S. A. Wilkinson, and M. J. Hartmann, Variational Hamiltonian simulation for translational invariant systems via classical pre-processing, arXiv:2106.03680 [quant-ph] (2021).
[41] E. H. Lieb and D. W. Robinson, The finite group velocity of quantum spin systems, Commun. Math. Phys. **28**, 251 (1972).
[42] G. Vidal, Efficient Classical Simulation of Slightly Entangled Quantum Computations, Phys. Rev. Lett. **91**, 147902 (2003).
[43] G. Vidal, Efficient Simulation of One-Dimensional Quantum Many-Body Systems, Phys. Rev. Lett. **93**, 040502 (2004).
[44] D. W. Robinson, Properties of propagation of quantum spin systems, ANZIAM J. **19**, 387 (1976).
[45] B. Nachtergaele and R. Sims, Lieb-Robinson bounds and the exponential clustering theorem, Commun. Math. Phys. **265**, 119 (2006).
[46] B. Nachtergaele, Y. Ogata, and R. Sims, Propagation of correlations in quantum lattice systems, J. Stat. Phys. **124**, 1 (2006).
[47] M. B. Hastings and T. Koma, Spectral gap and exponential decay of correlations, Commun. Math. Phys. **265**, 781 (2006).
[48] M. Foss-Feig, Z.-X. Gong, C. W. Clark, and A. V. Gorshkov, Nearly Linear Light Cones in Long-Range Interacting Quantum Systems, Phys. Rev. Lett. **114**, 157201 (2015).
[49] T. Matsuta, T. Koma, and S. Nakamura, Improving the Lieb-Robinson bound for long-range interactions, Ann. Henri Poincaré **18**, 519 (2017).
[50] D. V. Else, F. Machado, C. Nayak, and N. Y. Yao, Improved Lieb-Robinson bound for many-body Hamiltonians with power-law interactions, Phys. Rev. A **101**, 022333 (2020).
[51] T. Kuwahara and K. Saito, Strictly Linear Light Cones in Long-Range Interacting Systems of Arbitrary Dimensions, Phys. Rev. X **10**, 031010 (2020).
[52] M. C. Tran, A. Y. Guo, C. L. Baldwin, A. Ehrenberg, A. V. Gorshkov, and A. Lucas, Lieb-Robinson Light Cone for Power-Law Interactions, Phys. Rev. Lett. **127**, 160401 (2021).
[53] M. Horodecki, P. Horodecki, and R. Horodecki, General teleportation channel, singlet fraction, and quasidistillation, Phys. Rev. A **60**, 1888 (1999).
[54] M. A. Nielsen, A simple formula for the average gate fidelity of a quantum dynamical operation, Phys. Lett. A **303**, 249 (2002).
[55] M. B. Hastings, Light-cone matrix product, J. Math. Phys. **50**, 095207 (2009).
[56] U. Schollwöck, The density-matrix renormalization group in the age of matrix product states, Ann. Phys. **326**, 96 (2011).
[57] P. Virtanen, R. Gommers, Travis E. Oliphant, M. Haberland, T. Reddy, D. Cournapeau, E. Burovski, P. Peterson, W. Weckesser, J. Bright, *et al.*, SciPy 1.0: Fundamental algorithms for scientific computing in PYTHON, Nat. Methods **17**, 261 (2020).

[58] We also compute the stroboscopic dynamics under the same-depth Trotterization $V^{(L)}(\theta_{\mathrm{trot}}^{d=5})$. As the mean-square errors during $0 \leq t \leq 10\tau$, we obtain 3.72×10^{-5} for the initial state $|\psi_{\mathrm{LE}}^{(L)}(0)\rangle$ and 7.59×10^{-6} for $|\psi_{\mathrm{DW}}^{(L)}(0)\rangle$. They are accidentally comparable to the LVQC results by $V^{(L)}(\theta_{\mathrm{opt}})$, in spite of the relatively small average gate fidelity for $V^{(L)}(\theta_{\mathrm{trot}}^{d=5})$. This comes from the choice of initial states, since both the accurate time-evolution operator and the approximate one by Trotterization trivially act on the ferromagnetic regions by suppressing the errors.

[59] E. Knill and R. Laflamme, Power of One Bit of Quantum Information, Phys. Rev. Lett. **81**, 5672 (1998).

[60] J. Chow, O. Dial, and J. Gambetta, IBM quantum breaks the 100-qubit processor barrier, https://research.ibm.com/blog/127-qubit-quantum-processor-eagle (2021).

[61] S. Ebadi, A. Keesling, M. Cain, Tout T. Wang, H. Levine, D. Bluvstein, G. Semeghini, A. Omran, J. Liu, R. Samajdar, *et al.*, Quantum optimization of maximum independent set using Rydberg atom arrays, arXiv:2202.09372 [quant-ph] (2022).

[62] S. R. White and R. L. Martin, *Ab initio* quantum chemistry using the density matrix renormalization group, J. Chem. Phys. **110**, 4127 (1999).

[63] S. Wouters and D. Van Neck, The density matrix renormalization group for ab initio quantum chemistry, Eur. Phys. J. D **68**, 272 (2014).

[64] R. Zalesny, M. G. Papadopoulos, P. G. Mezey, and J. Leszczynski, *Linear-Scaling Techniques in Computational Chemistry and Physics: Methods and Applications*, Challenges and Advances in Computational Chemistry and Physics (Springer, 2011).

[65] D. Shepherd, Computation with unitaries and one pure qubit, arXiv:quant-ph/0608132 [quant-ph] (2006).

[66] P. W. Shor and S. P. Jordan, Estimating Jones polynomials is a complete problem for one clean qubit, arXiv:0707.2831 [quant-ph] (2007).

[67] K. Fujii, H. Kobayashi, T. Morimae, H. Nishimura, S. Tamate, and S. Tani, Impossibility of Classically Simulating One-Clean-Qubit Model with Multiplicative Error, Phys. Rev. Lett. **120**, 200502 (2018).